Molecular Pharmacology Fast Forward. Published on March 8, 2017 as DOI: 10.1124/mol.116.107870
This article has not been copyedited and formatted. The final version may differ from this version.

TITLE PAGE

Novel Thiosemicarbazones Inhibit Lysine-Rich CEACAM1 Co-isolated (LYRIC) and the LYRIC-Induced Epithelial-Mesenchymal Transition *via* Up-Regulation of N-Myc Downstream-Regulated Gene 1 (NDRG1)

Ruxing Xi, Ivan Ho Yuen Pun, Sharleen V. Menezes, Leyla Fouani, Danuta S. Kalinowski, Michael L.H. Huang, Xiaozhi Zhang, Des R. Richardson and Zaklina Kovacevic

Molecular Pharmacology and Pathology Program, Department of Pathology, University of Sydney, Sydney, New South Wales, Australia [R.X., I.H.Y.P., S.V.M., L.F., D.S.K., M.L.H., D.R.R., Z.K.].

Affiliations: *Department of Radiation Oncology, The First Affiliated Hospital of Xi'an Jiaotong University, China [R.X., X.Z]*.

Department of Applied Biology and Chemical Technology, the Hong Kong Polytechnic University, Hong Kong, China [I.H.Y.P.].

Molecular Pharmacology Fast Forward. Published on March 8, 2017 as DOI: 10.1124/mol.116.107870
This article has not been copyedited and formatted. The final version may differ from this version.

RUNNING TITLE PAGE

Running Title: Targeting NDRG1 to inhibit TNFα-mediated EMT and LYRIC.

Correspondence to: **Zaklina Kovacevic:** *Molecular Pharmacology and Pathology Program, Department of Pathology, University of Sydney, Sydney, New South Wales, Australia*. Tel: (61) 2 9651 6151; Email: zaklina.kovacevic@sydney.edu.au; **Des R. Richardson**: *Molecular Pharmacology and Pathology Program, Department of Pathology, University of Sydney, Sydney, New South Wales, Australia*. Tel: (61) 2 9036-6548; Fax (61) 2 9351-3429; Email: d.richardson@med.usyd.edu.au

Manuscript information:

Number of text pages: 46

Number of tables: 0

Number of figures: 11

Number of references: 61

Word count:

- Abstract: 249
- Introduction: 743
- Discussion: 1494

Abbreviations: AEG-1, astrocyte elevated gene-1; DFO, desferrioxamine; Dp44mT; di-2-pyridylketone 4,4-dimethyl-3-thiosemicarbazone; DpC, di-2-pyridylketone 4-cyclohexyl-4-methyl-3-thiosemicarbazone; EMT, epithelial to mesenchymal transition; HRP, horseradish peroxidase; IKK, IκB kinase; LYRIC, lysine-rich CEACAM1 co-isolated; MTDH, metadherin; NDRG1, N-myc down-stream regulated gene 1; NF-κB, nuclear factor-κB; PI3K, phosphatidylinositol 3-kinase; PTEN, phosphatase and tensin homolog; ROS, reactive oxygen species; TNFα, tumor necrosis factor α.

Molecular Pharmacology Fast Forward. Published on March 8, 2017 as DOI: 10.1124/mol.116.107870
This article has not been copyedited and formatted. The final version may differ from this version.

ABSTRACT

Tumor necrosis factor α (TNFα) plays a vital role in cancer progression, being associated with inflammation and promotion of cancer angiogenesis and metastasis. The effects of TNFα are mediated by its down-stream target, the oncogene, lysine-rich CEACAM1 co-isolated protein (LYRIC; also known as metadherin or astrocyte elevated gene-1). LYRIC plays an important role in activating the nuclear factor-κB (NF-κB) signaling pathway, which controls multiple cellular processes, including proliferation, apoptosis, migration, *etc*. In contrast, the metastasis suppressor, N-myc down-stream regulated gene 1 (NDRG1), has the opposite effect on the NF-κB pathway, being able to inhibit NF-κB activation and reduce angiogenesis, proliferation, migration and cancer cell invasion. These potent anti-cancer properties make NDRG1 an ideal therapeutic target. Indeed, a novel class of thiosemicarbazone anti-cancer agents that target this molecule have been developed, with the lead agent, di-2-pyridylketone 4-cyclohexyl-4-methyl-3-thiosemicarbazone (DpC), recently entering clinical trials for advanced and resistant cancers. To further elucidate the interaction between NDRG1 and oncogenic signaling, this study for the first time assessed the effects of NDRG1 on the tumorigenic properties of TNFα and its down-stream target, LYRIC. We demonstrate that NDRG1 inhibits the TNFα-mediated epithelial to mesenchymal transition (EMT). Further, NDRG1 also potently inhibited LYRIC expression, with a negative feedback loop existing between these two molecules. Examining the mechanism involved, we demonstrated that NDRG1 inhibited PI3K/AKT signaling, leading to reduced levels of the LYRIC transcriptional activator, c-Myc. Finally, we demonstrate that novel thiosemicarbazones that up-regulate NDRG1 also inhibit LYRIC expression, further highlighting their marked potential for cancer treatment.

Molecular Pharmacology Fast Forward. Published on March 8, 2017 as DOI: 10.1124/mol.116.107870
This article has not been copyedited and formatted. The final version may differ from this version.

INTRODUCTION

The cytokine, tumor necrosis factor α (TNFα), functions as a mediator of inflammation to promote angiogenesis, cancer progression and metastasis (Mochizuki et al., 2004, Wang and Lin, 2008, Balkwill, 2009). These effects are induced by one of its major down-stream targets, the transcription factor, nuclear factor-κB (NF-κB) (Karin and Greten, 2005, Karin, 2006, Wu et al., 2009). NF-κB signaling regulates genes involved in inflammation, the immune response, proliferation, migration and apoptosis (Bharti and Aggarwal, 2002).

TNFα facilitates NF-κB activation *via* up-regulation of lysine-rich CEACAM1 co-isolated protein (LYRIC), also known as metadherin (MTDH), or astrocyte elevated gene-1 (AEG-1) (Emdad et al., 2013, Wan et al., 2014). LYRIC was first identified as a TNFα-inducible transcript in human fetal astrocytes (Su et al., 2002, Su et al., 2003). The increased levels of LYRIC in response to TNFα were mediated by the phosphatidylinositol 3-kinase (PI3K) pathway, which promotes *LYRIC* transcription by mediating the direct binding of the transcription factor, c-Myc, to the *LYRIC* promoter (Lee et al., 2006).

LYRIC functions as an oncogene and is expressed in various cancers, including colorectal and prostate, where it is a poor prognostic factor (Emdad et al., 2006, Emdad et al., 2007, Li et al., 2008, Yoo et al., 2009, Wan et al., 2014). Furthermore, LYRIC plays a vital role in multiple biological processes *via* oncogenic signaling, with NF-κB being one of its main targets (Emdad et al., 2006, Emdad et al., 2013).

LYRIC activates the NF-κB pathway by facilitating degradation of the inhibitor of NF-κB (IκB), leading to release of the active p50/p65 NF-κB complex and its nuclear translocation (Emdad et al., 2006). In addition, LYRIC also directly binds to p65 NF-κB, acting as a

transcriptional co-activator and leading to increased transcription of genes, such as interleukin-8, which promotes the epithelial to mesenchymal transition (EMT), invasion and metastasis (Sarkar et al., 2008, Kalluri and Weinberg, 2009, Li et al., 2011). Moreover, LYRIC is directly phosphorylated and activated by the IκB kinase (IKK) at Ser298 (Krishnan et al., 2015). The NF-κB pathway also up-regulates LYRIC (Khuda et al., 2009), potentially due to cross-talk between the NF-κB and PI3K pathways (Hussain et al., 2012).

In contrast to LYRIC, the metastasis suppressor, N-myc down-stream regulated gene 1 (NDRG1), inhibits cancer progression (Fang et al., 2014). In fact, NDRG1 functions as a metastasis suppressor in multiple cancer-types (Shah et al., 2005, Ellen et al., 2008, Wangpu et al., 2015). NDRG1 negatively regulates the transforming growth factor-β (TGF-β)-mediated EMT by down-regulating the EMT marker, vimentin, while maintaining E-cadherin membrane localization (Chen et al., 2012). Recent investigations also demonstrated that NDRG1 negatively regulates oncogenic signaling mechanisms, including the Wnt-β-catenin, PI3K/AKT, TGF-β, Src and NF-κB pathways (Hosoi et al., 2009, Liu et al., 2012, Dixon et al., 2013, Kovacevic et al., 2013, Jin et al., 2014, Liu et al., 2015), as well as cell motility and migration (Sun et al., 2013, Wangpu et al., 2016).

Importantly, a novel class of anti-cancer agents was recently developed that chelate intracellular iron and potently up-regulate NDRG1 expression *via* hypoxia inducible factor-1α-dependent and -independent mechanisms (Le and Richardson, 2004, Whitnall et al., 2006, Kovacevic et al., 2011, Lane et al., 2013). These agents, namely di-2-pyridylketone 4,4-dimethyl-3-thiosemicarbazone (Dp44mT) and di-2-pyridylketone 4-cyclohexyl-4-methyl-3-thiosemicarbazone (DpC; **Fig. 1A**), bind iron and copper to form cytotoxic redox active complexes (Yuan et al., 2004, Richardson et al., 2006, Liu et al., 2015, Wangpu et al., 2015,

Molecular Pharmacology Fast Forward. Published on March 8, 2017 as DOI: 10.1124/mol.116.107870
This article has not been copyedited and formatted. The final version may differ from this version.

Stacy et al., 2016). The anti-cancer effects of Dp44mT and DpC were found to be mediated, at least in part, by their redox activity and ability to up-regulate NDRG1 (Chen et al., 2012, Liu et al., 2012, Sun et al., 2013, Liu et al., 2015). Indeed, Dp44mT has been reported to inhibit metastasis *in vivo,* with this effect being dependent on NDRG1 (Liu et al., 2012). Further, DpC recently entered multi-center clinical trials (NCT02688101) for advanced cancer (Jansson et al., 2015, Kalinowski et al., 2016), demonstrating their marked potential.

Considering the contrasting effects of NDRG1 and LYRIC on cancer progression and oncogenic signaling, this study for the first time examined the interaction between these molecules and the effect of NDRG1 on TNFα-mediated EMT. Further, the effects of the novel anti-cancer agents, Dp44mT and DpC, on LYRIC expression and downstream activity were also examined. We demonstrate that NDRG1, as well as Dp44mT and DpC, markedly inhibit LYRIC expression in prostate and colon cancer cells. These effects were mediated by a reduction in PI3K/c-Myc signaling, which led to inhibition of the oncogenic NF-κB pathway.

Molecular Pharmacology Fast Forward. Published on March 8, 2017 as DOI: 10.1124/mol.116.107870
This article has not been copyedited and formatted. The final version may differ from this version.

MATERIALS AND METHODS:

Cell Culture and Cell Treatments

Human prostate cancer DU145 cells were grown in RPMI 1640 medium (Sigma-Aldrich, St. Louis, MO, USA), while human colon cancer HT29 cells were grown in McCoy's 5A medium (Sigma-Aldrich). All media were supplemented with 10% fetal bovine serum (FBS, Sigma-Aldrich). NDRG1 over-expressing and silenced clones of the DU145 and HT29 cells were cultured and maintained, as described previously (Chen et al., 2012, Sun et al., 2013).

Human recombinant TNFα was obtained from PeproTech (Rocky Hill, NJ, USA; Cat.#: 300-01A) and used at a final concentration of 20 ng/mL for DU145 and HT29 cells. Both cell-types were treated with TNFα for 48 h/37ºC to induce the EMT. The thiosemicarbazones, DpC (**Fig.1 A**), Dp44mT (**Fig.1 A**) and the negative control compound, Bp2mT (**Fig.1 A**), were synthesized and characterized using standard methods (Richardson et al., 2006, Lovejoy et al., 2012, Stacy et al., 2016), while desferrioxamine (DFO, **Fig.1 A**) was purchased from Novartis (Basel, Switzerland). The agents, Bp2mT, DpC and Dp44mT, were dissolved in DMSO to generate 10 mM stocks, which were then further diluted in media containing 10% (v/v) FBS to a final concentration of 10 μM (final [DMSO] was ≤0.1% (v/v)). In contrast, DFO was dissolved in media containing 10% (v/v) FBS to a final concentration of 250 μM.

Protein Extraction and Western Blotting

Whole cell protein lysates were extracted using lysis buffer containing protease inhibitor (Cat.#: 1183617002; Roche Applied Science, Penzberg, Germany) and PhosSTOP (Cat.#: 04906845001; Roche Applied Science), as described previously (Kovacevic et al., 2008). Western blotting was performed using established protocols (Kovacevic et al., 2008). Primary antibodies used (diluted at 1:1,000-1:2,000) were against: NDRG1 (Cat.#: ab37897) and

Molecular Pharmacology Fast Forward. Published on March 8, 2017 as DOI: 10.1124/mol.116.107870
This article has not been copyedited and formatted. The final version may differ from this version.

LYRIC (Cat.#: ab168190) from Abcam (Cambridge, UK); and vimentin (Cat.#: 5741), NF-κB p65 (Cat.#: 4764), E-cadherin (Cat.#: 3195), PTEN (Cat.#: 9559), PI3K-p85 (Cat.#: 4257), PI3K-p110α/β/γ (Cat.#: 4249 (α); Cat.#: 3011 (β) and Cat.#: 5405 (γ)), AKT (Cat.#: 4685), p-AKT (Cat.#: 9271) and c-Myc (Cat.#: 5605) from Cell Signaling Technology (Beverly, MA, USA). The secondary antibodies implemented (diluted 1:10,000) include: horseradish peroxidase (HRP)–conjugated anti-goat (Cat.#: A5420), anti-rabbit (Cat.#: A6154) and anti-mouse (Cat.#: A4416) antibodies from Sigma-Aldrich.

Reverse Transcription Polymerase Chain Reaction (RT-PCR) and Reverse Transcription Quantitative PCR (RT-qPCR)

The mRNA expression of *NDRG1* and *LYRIC* in the DU145 and HT29 cell lines was assessed by RT-PCR and agarose gel electrophoresis. Approximately 1 x 10^6 cells from each cell line were seeded and incubated with either Bp2mT (10 μM), DpC (10 μM), Dp44mT (10 μM), or DFO (250 μM) for 24 h/37ºC. The RNA of each the cell line was extracted using the TRI-reagent (Applied Biosystems, Foster City, CA, USA; Cat. #: AM9738) according to the manufacturer's protocol. Using SuperScript® III One-Step RT-PCR System with Platinum® Taq DNA polymerase (Life Technologies, Carlsbad, CA, USA; Cat. #: 12574018), 0.12 μg of mRNA was amplified with primers against *NDRG1* and *LYRIC*, and examined by 1.5% agarose gel electrophoresis.

The mRNA expression of *NDRG1* and *LYRIC* was further confirmed by the SensiFAST SYBR No-ROX qPCR kit from Bioline (Eveleigh, NSW, Australia; Cat. #: BIO98002). RNA was first reverse-transcribed to cDNA by reverse-transcriptase from Promega (Madison, Wisconsin, USA; Cat.#: 1611244). qPCR reactions containing 50 ng of cDNA were conducted as follows: polymerase activation for 10 min at 95ºC; amplification for 40 cycles

Molecular Pharmacology Fast Forward. Published on March 8, 2017 as DOI: 10.1124/mol.116.107870
This article has not been copyedited and formatted. The final version may differ from this version.

with denaturation for 10 s at 95ºC and annealing/extension for 20 s at 60ºC. Melting curves were conducted to ascertain the specificity of the PCR product. The threshold cycle (Ct) was recorded to compare the change of expression by the $2^{\Delta Ct}$ method. The primers for *NDRG1* were: *5'-TCA CCC AGC ACT TTG CCG TCT-3'* (forward) and *5'-GCC ACA GTC CGC CAT CTT-3'* (reverse), while the primers for *LYRIC* were: *5'-GTT GAA GTG GCT GAG GGT-3'* (forward) and *5'-GGA AAT GAT GCG GTT GTA-3'* (reverse), and the primers for *β-actin* were: *5'-CCC GCC GCC AGC TCA CCA TGG-3'* (forward) and *5'-AAG GTC TCA AAC ATG ATC TGG GTC-3'* (reverse).

Cell Migration Assay

Cell migration was assessed using established transwell migration assays (Chen et al., 2012). Briefly, the quantitative migration assay was performed using the Cyto-Select™ 24-Well Cell Migration Assay kit from Corning (Corning, NY, USA), according to the manufacturer's protocol. In these studies, 5 x 10^4 cells in 200 μL serum-free medium were placed into the top chamber and 600 μL of 10% FBS containing medium was placed into the bottom chamber. After an incubation of 12 h/37ºC (DU145) or 36 h/37ºC (HT29) with TNFα (20 ng/mL), the cells that did not invade to the lower chamber were removed. The chambers were then stained with crystal violet for 20 min/room temperature. Stained cells adhering to the bottom of the chambers were observed and quantified by direct cell counting using a Zeiss AxioObserver Z1 fluorescence microscope (Carl-Zeiss AG, Oberkochen, Germany). At least five random fields per sample were selected for counting under the microscope.

Gene Silencing by Small Interfering RNA (siRNA)

Silencing LYRIC expression using siRNA was performed following the manufacturer's instructions. Briefly, at 60%-70% confluence, sh-NDRG1 and sh-Ctrl cells were transfected

Molecular Pharmacology Fast Forward. Published on March 8, 2017 as DOI: 10.1124/mol.116.107870
This article has not been copyedited and formatted. The final version may differ from this version.

with either LYRIC Silencer® Select siRNA duplexes (si-*LYRIC*; Cat.#: 4392420; 10 nM; Ambion, Thermo Fisher Scientific, Waltham, MA, USA) or the Silencer® Negative Control siRNA (si-Con; Cat.#: 4404021) at 10 nM using Lipofectamine 2000® (Invitrogen, Carlsbad, CA, USA). Following a 6 h/37ºC siRNA incubation, fresh medium was then added for a further 60 h/37ºC incubation. *c-Myc* was silenced in the sh-NDRG1 and sh-Ctrl cells using SignalSilence® siRNA (si-c-Myc; Car.#: 6341S; 100 pM; Cell Signaling Technology, Danvers, MA, USA) or the Negative Control siRNA (100 pM) using Lipofectamine RNAiMax (Invitrogen), with the cells being incubated with the siRNA for 24 h/37ºC, followed by fresh media for a further 24 h/37ºC.

Immunofluorescence

Immunofluorescence was performed to determine the co-localization between LYRIC and NF-κB p65 in DU145 and HT29 cell lines and their nuclear translocation in response to TNFα. In these experiments, 5×10^4 cells were seeded on glass cover slips and incubated with 20 ng/mL TNFα for 48 h/37ºC. The agents, Bp2mT (10 μM), Dp44mT (10 μM), DpC (10 μM), or DFO (250 μM), were added to the cells for the final 24 h/37ºC of TNFα treatment as described above. Following treatment, media was removed and the cells rinsed by PBS followed by 4% paraformaldehyde fixation. The cover slides were then treated with primary antibodies diluted 1:300 in 1% BSA in PBS for 24 h/4ºC. Two primary antibodies were used: anti-LYRIC antibody (Cat. #: ab124789) from Abcam; anti-NF-κB p65 antibody (Cat. #: 6956) from Cell Signaling Technology. After removal of the primary antibodies, the cells were incubated with anti-rabbit IgG 594 (Cat.#: 8889S) and anti-mouse IgG 488 (Cat.#: 4408S) conjugated secondary antibodies from Cell Signaling Technology for 1 h/room temperature. The coverslips were mounted onto slides using Pro-Long Gold anti-fade mounting solution containing 4',6-diamidino-2-phenylindole (DAPI; Invitrogen; Cat. #:

Molecular Pharmacology Fast Forward. Published on March 8, 2017 as DOI: 10.1124/mol.116.107870
This article has not been copyedited and formatted. The final version may differ from this version.

P36935). The slides were analyzed using a Zeiss fluorescent microscope described above equipped with an AxioCam camera and images were taken and analyzed using AxioVision software (Carl Zeiss AG, Oberkochen, Germany). Mander's overlap coefficient was determined using ImageJ (National Institutes of Health, Maryland, USA). The co-localization intensities presented in Figs. 5C, D and 6C, D were determined by examining the intensity value of LYRIC (C) or NF-κB (D) specifically in the area that is also expressing NF-κB (C) or DAPI (D) using ImageJ software.

Statistics

Data are mean ± standard deviation of at least 3 independent experiments and were compared using un-paired two-tailed Student's *t*-test (assuming unequal variance) or one-way ANOVA with Dunnett's multiple comparison post hoc test being used for comparing the treated groups with the control group. This was performed using GraphPad Prism 5.0 software (GraphPad Software, San Diego, CA, USA). Results were considered statistically significant only when $p < 0.05$.

Molecular Pharmacology Fast Forward. Published on March 8, 2017 as DOI: 10.1124/mol.116.107870
This article has not been copyedited and formatted. The final version may differ from this version.

RESULTS:

NDRG1 Over-Expression in HT29 and DU145 Cells Decreases LYRIC, while Silencing of NDRG1 Increases LYRIC Expression

In this study, we used two well-characterized cell-types: DU145 prostate cancer cells and HT29 colon cancer cells that stably over-express exogenous human NDRG1 (denoted "NDRG1") and compared the results to cells transfected with the empty vector control alone (denoted "Vector Ctrl"). To further complement these models, NDRG1-silenced clones (denoted "sh-NDRG1") of DU145 and HT29 cells were generated and compared to cells transfected with an empty control plasmid (denoted "sh-Ctrl"). These models were implemented as our previous studies using these cell-types have demonstrated that NDRG1 inhibits the EMT, cell migration and invasion (Chen et al., 2012, Sun et al., 2013, Jin et al., 2014, Liu et al., 2015, Wangpu et al., 2016).

Western blotting was utilized to detect LYRIC expression in the NDRG1 over-expressing and silenced clones of DU145 and HT29 cells. In both cell-types, we detected 2-3 NDRG1 bands with molecular weights of ~43 and 44 kDa, as described in previous studies (Chen et al., 2012, Sun et al., 2013, Jin et al., 2014, Liu et al., 2015, Wangpu et al., 2015, Wangpu et al., 2016). These bands have been suggested to correspond to phosphorylated or truncated NDRG1 protein, with the top band correlating with phosphorylated NDRG1 (Murakami et al., 2010, Ghalayini et al., 2013). Importantly, NDRG1 expression was significantly ($p < 0.001$) higher in the over-expressing clones relative to the Vector Ctrls (**Fig. 1B, C**), while the sh-NDRG1 clones demonstrated a significant ($p < 0.001$) decrease in NDRG1 expression relative to the sh-Ctrl cell-types (**Fig. 1B, C**).

Molecular Pharmacology Fast Forward. Published on March 8, 2017 as DOI: 10.1124/mol.116.107870
This article has not been copyedited and formatted. The final version may differ from this version.

Furthermore, NDRG1 over-expression in both cell-types resulted in a significant ($p < 0.001$-0.01) decrease in LYRIC expression, relative to Vector Ctrl cells (**Fig. 1B, C**). In contrast, NDRG1 silencing (sh-NDRG1) resulted in a significant ($p < 0.001$-0.01) increase in LYRIC expression when compared with the sh-Ctrl cells (**Fig. 1B, C**). These results demonstrate that NDRG1 inhibits LYRIC expression in DU145 and HT29 cells. Considering that LYRIC plays a vital role in cancer metastasis, further studies were focused on elucidating the relationship between NDRG1 and LYRIC.

Up-Regulation of NDRG1 Attenuated the TNFα-Mediated Expression of LYRIC and the EMT

Previous studies have shown that TNFα up-regulates the expression of LYRIC and promotes metastasis *via* its activation of the oncogenic NF-κB pathway (Su et al., 2003, Karin, 2006, Wu et al., 2009). Hence, we incubated both DU145 and HT29 cells with TNFα (20 ng/mL) for 48 h/37^{o}C to induce LYRIC expression and the EMT, and to determine the effect of NDRG1 over-expression or silencing on this process.

It is important to note that TNFα had no marked or significant ($p > 0.05$) effect on the expression of NDRG1 in either cell-type (**Fig. 2A, B**). However, upon the addition of TNFα, LYRIC expression was significantly ($p < 0.001$-0.01) increased in both DU145 and HT29 Vector Ctrl and sh-Ctrl cells (**Fig. 2A, B**). Interestingly, this effect was abolished in the NDRG1 over-expressing cells. In contrast, *NDRG1* silencing resulted in a more pronounced effect of TNFα on LYRIC expression in DU145, which was significantly ($p < 0.001$) increased in sh-NDRG1 DU145 cells relative to these cells not treated with TNFα (**Fig. 2A**). TNFα was also able to slightly and significantly ($p < 0.01$) increase LYRIC levels in the sh-NDRG1 HT29 cells, although not to the same extent as that observed using sh-Ctrl cells (**Fig.**

2B). The latter observation suggested that other factors could also influence the effect of TNFα on LYRIC in HT29 cells.

To further assess the effect of TNFα on down-stream signaling, NF-κB p65 was also examined in these cells as it is a central player in the oncogenic NF-κB pathway (Emdad et al., 2006). Similarly to LYRIC, TNFα also significantly (p < 0.001-0.05) increased NF-κB p65 levels in both DU145 and HT29 Vector Ctrl, sh-Ctrl and sh-NDRG1 cells, while this stimulatory effect was ablated by NDRG1 over-expression (**Fig. 2A, B**). Interestingly, the basal levels of p65 in the absence of TNFα were also markedly (p<0.05) reduced by NDRG1 over-expression in the DU145 cells (Fig. 2A), while there was no change in basal p65 in the HT29 cells (Fig. 2B). Moreover, silencing NDRG1 did not further alter the levels of p65 when compared to the sh-control cells for both DU145 and HT29 cell types.

Another TNFα down-stream target and marker of the EMT, namely vimentin (Ho et al., 2012), was also examined in both cell-types, with the same trend being observed, that is, TNFα significantly (p < 0.001-0.01) increased vimentin expression in Vector Ctrl, sh-Ctrl and sh-NDRG1 cells, while NDRG1 over-expression inhibited this effect (**Fig. 2A, B**).

Considering the role of NDRG1 and TNFα in modulating the EMT (Balkwill, 2009, Chen et al., 2012), the ability of these cells to migrate, which is an indication of metastatic potential (Kalluri and Weinberg, 2009), was then examined using transwell migration assays (**Fig. 2C, D**). These results demonstrate that TNFα significantly (p < 0.001) enhanced the migration of Vector Ctrl and sh-Ctrl DU145 and HT29 cells (**Fig. 2C, D**). Importantly, NDRG1 significantly (p < 0.001-0.01) inhibited this effect and decreased the migration of both DU145 and HT29 cells relative to the Vector Ctrl cells (**Fig. 2C**). On the other hand, *NDRG1*

Molecular Pharmacology Fast Forward. Published on March 8, 2017 as DOI: 10.1124/mol.116.107870
This article has not been copyedited and formatted. The final version may differ from this version.

silencing significantly ($p < 0.001$) increased migration of these cells, regardless of TNFα, relative to the sh-Ctrl (**Fig. 2D**).

In summary, the studies in **Fig. 2** indicate that NDRG1 inhibits the expression of down-stream targets of TNFα, namely LYRIC, NF-κB p65 and vimentin, and subsequently prevents the TNFα-mediated migration of both DU145 and HT29 cells.

Novel Thiosemicarbazones Decrease the Expression of LYRIC, while Up-Regulating NDRG1 in DU145 and HT29 Cells.

Studies from our laboratory and those of others reported that the novel thiosemicarbazones, namely DpC and Dp44mT, function as potent anti-tumor and anti-metastatic agents *in vitro* and *in vivo* (Yuan et al., 2004, Whitnall et al., 2006, Kovacevic et al., 2011, Liu et al., 2012, Lovejoy et al., 2012). Moreover, these agents also up-regulate the metastasis suppressor, NDRG1, *via* hypoxia inducible factor-1α-dependent and independent mechanisms in cancer cells by binding intracellular iron (Le and Richardson, 2004, Whitnall et al., 2006, Kovacevic et al., 2011, Lane et al., 2013, Sun et al., 2013). Considering the anti-tumor activity of these agents and also NDRG1, we further examined, for the first time, the effects of both DpC and Dp44mT on the mRNA and protein expression of LYRIC in DU145 and HT29 cells (**Fig. 3**). In addition to these agents, several control compounds were utilized. These included: **(1)** the negative control thiosemicarbazone, Bp2mT (**Fig. 1A**), which is incapable of chelating metal ions, and thus, cannot up-regulate NDRG1 (Yuan et al., 2004, Stacy et al., 2016, Wangpu et al., 2016); and **(2)** the well-characterized iron chelator, DFO (**Fig. 1A**), which binds iron with high affinity, but unlike Dp44mT and DpC, does not redox cycle (Kalinowski and Richardson, 2005). These control compounds were essential in order to determine whether the effects observed were due to iron depletion or redox activity. All cell-types were

Molecular Pharmacology Fast Forward. Published on March 8, 2017 as DOI: 10.1124/mol.116.107870
This article has not been copyedited and formatted. The final version may differ from this version.

incubated with either: Bp2mT (10 μM), DFO (250 μM), Dp44mT (10 μM), or DpC (10 μM) for 24 h/37^{o}C. Notably, DFO was utilized at 250 μM due to its low membrane permeability and meagre iron chelation efficacy (Yuan et al., 2004).

The mRNA levels of *NDRG1* and *LYRIC* were assessed in both DU145 and HT29 cells. As reported previously (Le and Richardson, 2004, Whitnall et al., 2006), the mRNA levels of *NDRG1* were significantly ($p < 0.001$) up-regulated in response to DFO, Dp44mT, or DpC in both cell-types, as shown by both RT-PCR (**Fig. 3A, B**) and RT-qPCR (**Fig. 3C, D**), while the negative control, Bp2mT, had no significant ($p > 0.05$) effect. Conversely, the mRNA levels of *LYRIC* were significantly ($p < 0.001$) reduced by Dp44mT and DpC in both cell-types (**Fig. 3A-D**). Notably, DFO was also able to significantly ($p < 0.001$) reduce *LYRIC* mRNA expression in HT29 cells (**Fig. 3B, D**), while having no marked effect in the DU145 cells (**Fig. 3A, C**). Overall, these results demonstrate that Dp44mT and DpC up-regulate *NDRG1* mRNA levels and also down-regulate *LYRIC* mRNA expression in the cells assessed.

To determine the effect of these agents on the protein levels of NDRG1 and LYRIC, western blot analysis was then performed. Examining both DU145 (**Fig. 3E**) and HT29 (**Fig. 3F**) cells, the expression of NDRG1 was not significantly ($p > 0.05$) affected by Bp2mT when compared to the untreated control. However, DFO, DpC and Dp44mT all caused a pronounced and significant ($p < 0.001$) increase in NDRG1 expression, as described previously (Chen et al., 2012, Sun et al., 2013). Moreover, DFO, DpC and Dp44mT also significantly ($p < 0.01$-0.001) reduced the expression of LYRIC relative to the control in both cell-types (**Fig. 3E, F**). Hence, in good agreement with the mRNA levels described above, Dp44mT and DpC markedly up-regulate NDRG1, while reducing LYRIC protein levels in both DU145 and HT29 cells. Interestingly, while DFO reduced both *LYRIC* mRNA and

Molecular Pharmacology Fast Forward. Published on March 8, 2017 as DOI: 10.1124/mol.116.107870
This article has not been copyedited and formatted. The final version may differ from this version.

protein levels in HT29 cells, when examining DU145 cells, this agent was only able to reduce LYRIC protein levels, suggesting that the post-transcriptional processing of LYRIC, rather than its transcription, was affected in this cell-type by DFO.

Thiosemicarbazones Attenuate TNFα-Induced LYRIC, NF-κB p65 and Vimentin Expression in DU145 and HT29 Cells

Considering the ability of DFO, Dp44mT and DpC to generally reduce both the mRNA and protein levels of LYRIC, further studies then assessed whether these agents could affect the TNFα-mediated effects on LYRIC, as well as its down-stream effectors, namely NF-κB p65 and vimentin. In these studies, DU145 and HT29 cells were incubated with TNFα for 48 h/37ºC, with the addition of either: Bp2mT (10 μM), Dp44mT (10 μM), DpC (10 μM), or DFO (250 μM), occurring in the final 24 h of the incubation (**Fig. 4**).

As shown in **Fig.4**, NDRG1 was significantly ($p < 0.001$) increased in both cell-types relative to the Control following incubation with either DFO, DpC, or Dp44mT, regardless of TNFα treatment. In contrast, as described above, LYRIC was significantly ($p < 0.001$-0.05) increased after TNFα treatment in the Control, Bp2mT and DFO-treated cells. However, when combined with Dp44mT or DpC, the TNFα-induced increase of LYRIC was completely attenuated in both cell-types (**Fig. 4A and B**). Further, NF-κB p65 was also significantly ($p < 0.001$-0.05) increased after TNFα treatment in Control, Bp2mT and DFO-treated cells, while DpC and Dp44mT attenuated the increase of NF-κB p65 by TNFα in both cell-types (**Fig. 4A, B**). Notably, the basal levels of NF-κB p65 were unaffected by Dp44mT and DpC in these cells, with the exception of DpC-treated DU145 cells, which showed a slight increase in basal NF-κB p65 when compared to the controls.

Molecular Pharmacology Fast Forward. Published on March 8, 2017 as DOI: 10.1124/mol.116.107870
This article has not been copyedited and formatted. The final version may differ from this version.

Considering these results above, it is notable that while DFO, DpC and Dp44mT all bind intracellular metals, only DpC and Dp44mT are also able to form redox active complexes, leading to the generation of reactive oxygen species (ROS) (Yuan et al., 2004, Richardson et al., 2006, Lovejoy et al., 2012, Stacy et al., 2016). This observation suggested that the redox activity of DpC and Dp44mT may have attenuated TNFα-induced LYRIC expression through the inhibition of NF-κB p65 activity, as this latter molecule is redox-sensitive (Flohe et al., 1997) and can also affect LYRIC levels (Khuda et al., 2009). A similar trend in the effects of these agents on protein expression was also observed with vimentin, with a significant ($p <$ 0.001-0.01) increase being observed after TNFα treatment in Control and Bp2mT-treated cells, while DFO, DpC and Dp44mT were able to attenuate the TNFα-mediated increase in both cell-types. In this latter case, the results could possibly be explained by the ability of DFO, DpC and Dp44mT to up-regulate NDRG1, which is known to prevent the EMT and inhibit vimentin expression (Chen et al., 2012).

Taken together, these results demonstrate that Dp44mT and DpC inhibit the TNFα-mediated effects of LYRIC, NF-κB p65 and vimentin, while these thiosemicarbazones and also DFO were able to inhibit the effect of this cytokine on vimentin expression.

The Nuclear Localization of NF-κB p65 and its Co-Localization with LYRIC is Attenuated by DpC and Dp44mT in DU145 and HT29 Cells

Following on from these studies assessing the effect of the novel thiosemicarbazones on TNFα-mediated LYRIC and NF-κB p65 expression, we next examined the cellular localization of these proteins, as their nuclear translocation is vital for their function (Emdad et al., 2006, Karin, 2006, Emdad et al., 2007, Sarkar et al., 2008, Emdad et al., 2013, Sarkar and Fisher, 2013). Importantly, the co-localization between NF-κB p65 and LYRIC, which

Molecular Pharmacology Fast Forward. Published on March 8, 2017 as DOI: 10.1124/mol.116.107870
This article has not been copyedited and formatted. The final version may differ from this version.

occurs in response to TNFα (Emdad et al., 2006, Emdad et al., 2007, Sarkar et al., 2008, Emdad et al., 2013, Sarkar and Fisher, 2013) was also assessed by immunofluorescence in the presence of the DFO, DpC and Dp44mT, as well as the negative control compound, Bp2mT, in both DU145 and HT29 cells (**Figs. 5, 6**).

Upon examining DU145 cells, LYRIC (red fluorescence) and NF-κB p65 (green fluorescence) were co-localized (leading to yellow fluorescence) in both the untreated (**Fig. 5A**) and the TNFα-treated cells (**Fig. 5B**). In fact, TNFα further promoted the co-localization of these molecules as judged by the increase in the Mander's co-localization coefficient for LYRIC/NF-κB p65 which increased from 0.799 to 0.824 in the absence and presence of TNFα, respectively (**Fig. 5A, B**). Notably, the co-localization between NF-κB p65 and LYRIC was markedly reduced in the presence of DFO, Dp44mT, or DpC in both the untreated and TNFα-treated cells (**Fig. 5A, B**) and this was found to be significant ($p < 0.001$-0.05) upon assessment of the co-localization intensity (**Fig. 5C**). Considering that NF-κB p65 exerts its function in the nucleus, the co-localization intensity (**Fig. 5D**) between NF-κB p65 and DAPI (nuclear marker) was also assessed from the images in **Fig. 5A and B**. Interestingly, the nuclear levels of NF-κB p65 were also significantly ($p < 0.001$) reduced by DFO, DpC, or Dp44mT in the untreated cells, while DFO or Dp44mT also significantly ($p <$ 0.01-0.05) reduced nuclear NF-κB p65 in the TNFα-treated DU145 cells (**Fig. 5D**).

A similar general trend was also observed examining HT29 cells (**Fig. 6**), where DFO, DpC, or Dp44mT significantly ($p < 0.001$) reduced the co-localization between NF-κB p65 and LYRIC in both the absence and presence of TNFα (**Fig. 6A, B, C**). Further, the nuclear localization of NF-κB p65 was also significantly ($p < 0.001$-0.01) reduced by all three agents

Molecular Pharmacology Fast Forward. Published on March 8, 2017 as DOI: 10.1124/mol.116.107870
This article has not been copyedited and formatted. The final version may differ from this version.

in untreated HT29 cells, while in the TNFα-treated cells, DpC and Dp44mT significantly ($p <$ 0.01) decreased nuclear NF-κB p65 (**Fig. 6D**).

Overall, these results clearly demonstrate the inhibitory effect of DFO, DpC and Dp44mT on the co-localization of NF-κB p65 with LYRIC, as well as its nuclear translocation. These results are consistent with the ability of these agents to inhibit the TNFα-mediated increase in vimentin (**Fig. 4**), and their ability to inhibit the EMT, migration and also the invasion of these cell-types (Chen et al., 2012, Sun et al., 2013, Liu et al., 2015, Wangpu et al., 2016).

NDRG1 Plays an Important Role in the Ability of Novel Thiosemicarbazones to Inhibit LYRIC Expression in HT29 Cells.

To determine whether the inhibitory effects of DFO, DpC, or Dp44mT on LYRIC (**Figs. 3-5**) were mediated by NDRG1, studies using DU145 and HT29 cells stably transfected with *NDRG1* shRNA (sh-NDRG1) and their corresponding control cells (sh-Ctrl) were incubated for 24 h/37ºC with either: DFO (250 μM), DpC (10 μM), Dp44mT (10 μM), or the negative control, Bp2mT (10 μM), and the expression of LYRIC was examined (**Fig. 7**). In DU145 sh-NDRG1 cells, while NDRG1 was significantly ($p <$ 0.001) reduced in the control-treated cells relative to sh-Ctrl-treated control, DFO, DpC and Dp44mT still significantly ($p <$ 0.001) up-regulated NDRG1 expression to a similar degree to that of the DU145 sh-Ctrl cells (**Fig. 7A**). This observation suggested that these agents overcame the silencing of NDRG1 in this cell-type. Hence, the ability of DFO, DpC and Dp44mT to down-regulate LYRIC was similar in both sh-Ctrl and sh-NDRG1 cells (**Fig. 7A**).

Molecular Pharmacology Fast Forward. Published on March 8, 2017 as DOI: 10.1124/mol.116.107870
This article has not been copyedited and formatted. The final version may differ from this version.

However, in the HT29 sh-NDRG1 cells, the levels of NDRG1 were markedly (p < 0.001-0.01) lower overall when compared to the sh-Ctrl, even in the presence of DFO, Dp44mT or DpC (**Fig. 7B**). Consequently, while these agents were still able to significantly (p < 0.01-0.05) decrease LYRIC in both sh-Ctrl and sh-NDRG1 cells, their inhibitory effect on LYRIC expression was markedly (p < 0.001) lower in the sh-NDRG1 cells when compared to the sh-Ctrl cells. This finding suggested that NDRG1 plays a major role in the ability of these agents to inhibit LYRIC expression.

The difference between DU145 and HT29 cells in responding to the effects of sh-NDRG1 is probably due to the varied response of these different tumor cell-types to silencing and to the agents examined. Nevertheless, these results further indicate that DpC and Dp44mT decrease LYRIC expression, at least in part, through up-regulation of NDRG1.

LYRIC Levels can also Influence NDRG1 Expression in DU145 and HT29 Cells.

To gain further insights into the interrelationship between the activities of NDRG1 and LYRIC, we conducted studies to examine whether LYRIC itself is able to modulate NDRG1 expression. In these studies, *LYRIC* siRNA (si-LYRIC), or a non-specific control siRNA (si-Ctrl) were transiently transfected into both sh-Ctrl and sh-NDRG1 DU145 and HT29 cells and the levels of both NDRG1 and LYRIC examined (**Fig. 7C, D**).

As shown in **Fig. 7C and D**, after si-LYRIC was added to sh-Ctrl or sh-NDRG1 DU145 and HT29 cells, there was a significant (p < 0.001-0.01) increase in NDRG1 levels, which occurred due to the significant (p < 0.001-0.01) decrease in LYRIC in both cell-types relative to the si-Ctrl cells (**Fig. 7C, D**). This observation suggests that LYRIC itself suppresses

Molecular Pharmacology Fast Forward. Published on March 8, 2017 as DOI: 10.1124/mol.116.107870
This article has not been copyedited and formatted. The final version may differ from this version.

NDRG1 expression and indicates the existence of a negative feedback loop between these two molecules.

Effect of NDRG1 on the Up-Stream Regulators of LYRIC: NDRG1 Inhibits the PI3K Pathway and its Down-stream Target, c-Myc

To investigate the potential mechanisms involved in the NDRG1-mediated effects on LYRIC, further studies focused on the major up-stream regulator of LYRIC expression, namely the PI3K pathway (Lee et al., 2006, Emdad et al., 2013). Once activated in response to stimuli such as TNFα, PI3K (consisting of a p85 regulatory subunit and p110α/β/γ catalytic subunits) facilitates the phosphorylation of phosphatidylinositol-4,5-bisphosphate (PIP2) to phosphatidylinositol-3,4,5-trisphosphate (PIP3), which subsequently leads to the phosphorylation and activation of AKT (Liu et al., 2009). Activated AKT ultimately promotes the function of the transcription factor, c-Myc, that directly binds to the *LYRIC* promoter, increasing the expression of this molecule (Lee et al., 2006, Zhu et al., 2008). Further, a potent inhibitor of the PI3K pathway, namely phosphatase and tensin homolog (PTEN), was demonstrated to suppress LYRIC levels (Lee et al., 2006). Importantly, our laboratory previously demonstrated that NDRG1 promotes PTEN expression and has an inhibitory effect on the PI3K pathway (Dixon et al., 2013, Kovacevic et al., 2013). Hence, we hypothesized that this may be the mechanism behind its inhibitory activity on LYRIC.

To this end, we examined the effect of NDRG1 over-expression (**Fig. 8A**) as well as *NDRG1* silencing (**Fig. 8B**) on key molecules involved in the PI3K pathway, namely PI3K-p85, p-AKT, AKT, c-Myc and PTEN in DU145 cells in the presence and absence of TNFα. As shown in **Fig. 8A**, TNFα treatment of the Vector Ctrl cells led to no significant ($p > 0.05$)

Molecular Pharmacology Fast Forward. Published on March 8, 2017 as DOI: 10.1124/mol.116.107870
This article has not been copyedited and formatted. The final version may differ from this version.

effect on NDRG1, PI3K-p85, p-AKT, c-Myc, or PTEN levels, but resulted in a significant ($p < 0.01$) increase in total AKT expression. Importantly, the marked and significant ($p < 0.001$) over-expression of NDRG1 in DU145 cells led to a significant ($p < 0.001$-0.05) decrease in PI3K-p85, p-AKT and c-Myc levels, regardless of TNFα, while NDRG1 significantly ($p < 0.01$) up-regulated PTEN in the absence of TNFα (**Fig. 8A**). The opposite trend was generally observed in DU145 cells transfected with sh-NDRG1 (**Fig. 8B**), where in the presence of TNFα, the suppression of NDRG1 either significantly ($p < 0.05$) increased p-AKT and c-Myc, or slightly increased PI3K-p85 relative to the sh-Ctrl. Furthermore, transfection of DU145 cells with sh-NDRG1 also resulted in either a significant ($p < 0.05$) decrease, or slight decrease in PTEN expression in the absence or presence of TNFα, respectively (**Fig. 8B**). Notably, PI3K-p110α/β/γ levels were not significantly ($p > 0.05$) affected by NDRG1 over-expression or silencing in DU145 cells (data not shown).

Similarly, examining HT29 cells (**Fig. 9A**), NDRG1 over-expression also led to significantly ($p < 0.001$) reduced pAKT and c-Myc levels, while significantly ($p < 0.01$) up-regulating PTEN expression, irrespective of TNFα treatment. In contrast, silencing *NDRG1* in HT29 cells led to significantly ($p < 0.001$) greater PI3K-p85 levels regardless of TNFα, as well as significantly ($p < 0.001$-0.05) increased p-AKT and c-Myc levels particularly in the presence of TNFα. Furthermore, silencing *NDRG1* also significantly ($p < 0.05$) potentiated the TNFα-mediated reduction of PTEN (**Fig. 9B**). Again, as found using DU145 cells above, PI3K-p110α/β/γ levels were not significantly ($p > 0.05$) affected by NDRG1 over-expression or silencing in HT29 cells (data not shown).

Molecular Pharmacology Fast Forward. Published on March 8, 2017 as DOI: 10.1124/mol.116.107870
This article has not been copyedited and formatted. The final version may differ from this version.

Overall, these results suggest that NDRG1 has an inhibitory effect on the PI3K pathway and its down-stream target, c-Myc, which may be responsible for the reduced LYRIC levels mediated by NDRG1.

NDRG1 Regulates LYRIC Expression via its Effects on c-Myc

As demonstrated above, the effects of the metastasis suppressor, NDRG1, on LYRIC may be mediated by the inhibition of c-Myc expression (**Figs. 8-9**). To further examine this hypothesis, we utilized siRNA specific for *c-Myc* (si-c-Myc) to silence this latter transcription factor in DU145 cells and assessed whether *NDRG1* silencing could still lead to up-regulation of LYRIC. In these studies, the sh-Ctrl or sh-NDRG1 DU145 cells were used and transiently transfected with either control siRNA, or si-c-Myc.

The expression of NDRG1 was markedly ($p < 0.01$-0.05) reduced in the sh-NDRG1 cells when compared to the sh-Ctrl cells regardless of si-c-Myc (**Fig. 9C**). As expected, the expression of c-Myc was significantly ($p < 0.05$) reduced in both sh-Ctrl and sh-NDRG1 cells following treatment with si-c-Myc (**Fig. 9C**). Further, after treatment with control siRNA, c-Myc expression was significantly ($p < 0.05$) increased in sh-NDRG1 cells, when compared to sh-Ctrl cells. Conversely, silencing *c-Myc* also led to significantly ($p < 0.05$) increased levels of NDRG1 in the sh-Ctrl cells, which has previously been reported (Zhang et al., 2008), suggesting a negative feedback loop exists between these two molecules.

Examining the expression of LYRIC in these cells, no marked effect of silencing *c-Myc* was observed in the sh-Ctrl cells (**Fig. 9C**). In the sh-NDRG1 cells, LYRIC levels were significantly ($p < 0.01$) increased when compared to the sh-Ctrl, as was demonstrated in **Fig. 1B**. This finding again confirms the inhibitory effect of NDRG1 on LYRIC expression.

Molecular Pharmacology Fast Forward. Published on March 8, 2017 as DOI: 10.1124/mol.116.107870
This article has not been copyedited and formatted. The final version may differ from this version.

Notably, this increase in LYRIC was completely abolished upon silencing *c-Myc* in sh-NDRG1 cells, and in fact, resulted in a significant ($p < 0.05$) decrease in LYRIC expression relative to the si-Ctrl in sh-NDRG1 cells (**Fig. 9C**). This observation suggests that c-Myc plays a role in the up-regulation of LYRIC in response to *NDRG1* silencing, and further implies that NDRG1 inhibits LYRIC expression *via* its inhibitory effect on c-Myc.

Effect of the Novel Thiosemicarbazones on the PI3K Pathway and c-Myc

Considering our results demonstrating the inhibitory effect of NDRG1 on the PI3K pathway and c-Myc expression (**Fig. 8 and 9**), we further assessed the effect of DFO, Dp44mT and DpC (relative to the negative control agent, Bp2mT; (Stacy et al., 2016, Wangpu et al., 2016)) on these important regulators of LYRIC expression in both DU145 and HT29 cells. This was particularly important to examine in terms of dissecting the mechanism involved in the ability of these agents to up-regulate NDRG1 levels and reduce LYRIC expression (**Fig. 3**).

Examining PI3K-p85, this molecule was only significantly ($p < 0.01$) reduced by Dp44mT in the DU145 cells (**Fig. 10A**), while DFO, DpC and Dp44mT significantly ($p < 0.001$-0.01) reduced its expression in HT29 cells (**Fig. 10B**). Incubation of both these cell-types with DFO, DpC, or Dp44mT was accompanied by a significant ($p < 0.001$-0.01) reduction in p-AKT levels relative to the control, while total AKT expression was only significantly ($p < 0.001$-0.05) reduced by DFO and Dp44mT (**Fig. 10A, B**). Both DpC and Dp44mT also significantly ($p < 0.001$-0.01) reduced c-Myc levels in both cell-types, while the effect of DFO on decreasing c-Myc expression was only significant ($p < 0.001$) in HT29 cells (**Fig. 10B**). Finally, PTEN expression was significantly ($p < 0.001$-0.01) increased in DU145 cells by DFO, DpC and Dp44mT (**Fig. 10A**), while DpC and Dp44mT also significantly ($p < 0.001$-0.05) increased PTEN in HT29 cells (**Fig. 10B**).

Molecular Pharmacology Fast Forward. Published on March 8, 2017 as DOI: 10.1124/mol.116.107870
This article has not been copyedited and formatted. The final version may differ from this version.

In summary, DFO, Dp44mT and DpC generally inhibit the PI3K pathway and c-Myc, while promoting PTEN expression, which could account for their ability to inhibit *LYRIC* mRNA and protein levels.

Molecular Pharmacology Fast Forward. Published on March 8, 2017 as DOI: 10.1124/mol.116.107870
This article has not been copyedited and formatted. The final version may differ from this version.

DISCUSSION

LYRIC is up-regulated in a wide variety of cancers and contributes to cancer progression and metastatic development (Emdad et al., 2013, Sarkar and Fisher, 2013, Shi and Wang, 2015). This molecule is also regulated by a number of major oncogenic signaling pathways including PI3K/AKT, NF-κB, *etc.* (Emdad et al., 2013, Sarkar and Fisher, 2013, Shi and Wang, 2015). We and others recently discovered that the metastasis suppressor, NDRG1, functions to inhibit these latter oncogenic signaling pathways and subsequently attenuates cancer progression and the metastatic cascade (Hosoi et al., 2009, Chen et al., 2012, Liu et al., 2012, Dixon et al., 2013, Kovacevic et al., 2013, Jin et al., 2014, Wangpu et al., 2016). Further, our group has developed a novel class of anti-cancer agents, namely Dp44mT and DpC, which markedly up-regulate NDRG1 and potently inhibit oncogenic signaling pathways, cancer cell proliferation and metastasis (Le and Richardson, 2004, Whitnall et al., 2006, Kovacevic et al., 2011, Chen et al., 2012, Liu et al., 2012, Lovejoy et al., 2012, Dixon et al., 2013, Sun et al., 2013, Wangpu et al., 2016). As part of their biological activity, these thiosemicarbazones are known to block the EMT, inhibit cellular properties required for metastasis *in vitro* (*e.g.*, cellular migration), and also reduce metastasis *in vivo via* their ability to up-regulate NDRG1 (Chen et al., 2012, Liu et al., 2012, Sun et al., 2013, Liu et al., 2015, Wangpu et al., 2016).

To this end, the current study examined, for the first time, the effects of NDRG1 on the expression of LYRIC. We demonstrate that NDRG1 is a potent suppressor of LYRIC, with the up-regulation of NDRG1 markedly reducing LYRIC expression levels, while silencing *NDRG1* increased LYRIC. Interestingly, LYRIC itself was also able to regulate NDRG1 expression, with the silencing of *LYRIC* leading to markedly greater NDRG1 levels. This observation suggested that a negative feedback loop exists between these two molecules.

Molecular Pharmacology Fast Forward. Published on March 8, 2017 as DOI: 10.1124/mol.116.107870
This article has not been copyedited and formatted. The final version may differ from this version.

It has been reported that LYRIC expression is up-regulated by the PI3K/AKT signaling pathway *via* the transcription factor, c-Myc, which directly binds to the *LYRIC* promoter (Lee et al., 2006) (**Fig. 11**). This oncogenic signaling pathway is stimulated by the ligand, TNFα (Kang et al., 2005, Lee et al., 2006). In the current investigation, while TNFα increased LYRIC levels, NDRG1 was able to completely inhibit this effect. Further, NDRG1 also inhibited key molecules involved in the PI3K/AKT pathway, including: ***(i)*** PI3K-p85; ***(ii)*** p-AKT, and; ***(iii)*** c-Myc in both DU145 and HT-29 cells. This effect was accompanied by a marked increase in the PI3K/AKT inhibitor, PTEN, in response to NDRG1 over-expression. These results are in good agreement with previous studies from our laboratory demonstrating the inhibitory effect of NDRG1 on the PI3K/AKT pathway (Dixon et al., 2013, Kovacevic et al., 2013), and indicate that NDRG1 may inhibit LYRIC expression *via* this particular mechanism. In fact, we further confirmed the importance of c-Myc in the NDRG1-mediated effect on LYRIC by using *c-Myc* siRNA, demonstrating that NDRG1 inhibits LYRIC expression *via* its negative regulation of c-Myc.

Notably, as well as being down-stream of the PI3K/AKT pathway, LYRIC itself is also able to activate this pathway (Lee et al., 2008). In fact, LYRIC can increase phosphorylation of both AKT and GSK3β, subsequently leading to c-Myc stabilization, creating a positive feed-back loop (Lee et al., 2008). Our studies indicate that NDRG1 can potentially disrupt this positive feedback loop by reducing p-AKT and c-Myc levels, although whether this is mediated by the reduction of LYRIC, or if this is responsible for reduced LYRIC levels remains to be determined.

Molecular Pharmacology Fast Forward. Published on March 8, 2017 as DOI: 10.1124/mol.116.107870
This article has not been copyedited and formatted. The final version may differ from this version.

In addition to assessing the effect of NDRG1 on LYRIC, we also examined a novel class of anti-cancer agents that can potently up-regulate NDRG1 in tumor cells, namely Dp44mT and DpC (Le and Richardson, 2004, Whitnall et al., 2006, Kovacevic et al., 2011), and the effects of these agents on LYRIC. In fact, DpC has recently entered Phase I clinical trials for the treatment of advanced and resistant tumors (NCT02688101) (Jansson et al., 2015, Kalinowski et al., 2016), with this agent demonstrating pronounced efficacy and selectivity in multiple cancer-types *in vitro* and *in vivo* (Kovacevic et al., 2011, Lovejoy et al., 2012, Guo et al., 2016, Seebacher et al., 2016, Seebacher et al., 2016). Consistent with their ability to up-regulate NDRG1, both Dp44mT and DpC also significantly reduced *LYRIC* mRNA as well as its protein levels. Further, these thiosemicarbazones also completely inhibited the TNFα-mediated increase in LYRIC levels. These effects were found to be dependent on NDRG1 in HT29 cells as *NDRG1* silencing markedly reduced the ability of these agents to decrease LYRIC. In DU145 cells, despite silencing *NDRG1*, DpC and Dp44mT were still able to increase the levels of this metastasis suppressor and subsequently reduced LYRIC to the same extent as in the control cells. This may be due to these agents overwhelming the effect of the *NDRG1* shRNA in this cell-type, as has been observed previously (Sun et al., 2013, Wangpu et al., 2016).

Similarly to NDRG1, Dp44mT and DpC were also able to inhibit the major activating pathway of LYRIC, namely the PI3K/AKT pathway, leading to reduced levels of pAKT and c-Myc in both cell-types, while PI3K-p85 was only reduced in the HT29 cells. Further, PTEN was significantly up-regulated by these thiosemicarbazones in both DU145 and HT29 cells, further suggesting that inhibition of the PI3K/AKT pathway plays a key role in the ability of these compounds to inhibit LYRIC (**Fig. 11**). Considering this, additional studies directly assessing the importance of AKT in the activity of these novel agents could be potentially

warranted. For example, genetic manipulation of AKT (*e.g.*, ectopic expression of AKT) could provide information about the functional role of this protein in the response to thiosemicarbazones. However, as AKT is not the direct activator of LYRIC, with this effect being actually mediated *via* c-Myc (Lee et al., 2006), our studies focused on establishing the importance of c-Myc on NDRG1-mediated LYRIC expression, which was confirmed (**Fig. 9C**).

LYRIC functions to activate and promote a number of oncogenic signaling pathways, with NF-κB being its major target (Emdad et al., 2006, Sarkar et al., 2008). In response to TNFα, LYRIC was found to bind NF-κB p65 and translocate to the nucleus, leading to transcriptional activation of genes controlling cell proliferation and invasion (Emdad et al., 2006). Herein, we demonstrate that Dp44mT and DpC significantly inhibited the levels of NF-κB p65, as well as its nuclear co-localization with LYRIC in both cell-types examined (**Fig. 11**). Notably, a recent study has demonstrated that the IKK complex can phosphorylate LYRIC, leading to its activation (Krishnan et al., 2015). Our studies demonstrating an inhibitory effect of NDRG1 on LYRIC are further supported by previous findings, which showed that NDRG1 can also reduce the expression of IKKβ, a component of the IKK complex (Hosoi et al., 2009). Hence, NDRG1 may also potentially inhibit LYRIC phosphorylation and activity, although this requires further assessment.

It is important to note that LYRIC has also been shown to promote the EMT in cancer cells (Wang et al., 2016). We also demonstrated that Dp44mT and DpC inhibits characteristics of the EMT in DU145 and HT-29 cells *via* their effects on NDRG1 (Chen et al., 2012), leading to inhibition of cell migration and invasion. Considering this, the current study also assessed the activity of TNFα on the invasive ability of DU145 and HT-29 cells, showing that this

Molecular Pharmacology Fast Forward. Published on March 8, 2017 as DOI: 10.1124/mol.116.107870
This article has not been copyedited and formatted. The final version may differ from this version.

cytokine promoted a significant increase in their migration. This effect was inhibited in response to NDRG1 over-expression, or enhanced in response to *NDRG1* silencing. Together, these results indicate that NDRG1 and the novel anti-cancer agents, Dp44mT and DpC, may inhibit the EMT, at least in part, *via* their effects on LYRIC and TNFα signaling.

Considering the anti-cancer activity of Dp44mT and DpC, while NDRG1 plays a major role in their anti-metastatic effects (Chen et al., 2012, Liu et al., 2012, Sun et al., 2013, Liu et al., 2015, Wangpu et al., 2016), it is important to note that these agents also have other mechanisms of action which include the production of ROS and the sequestration of iron (Jansson et al., 2015). While the current study demonstrates that the effect of these agents on LYRIC are mediated by NDRG1, their other mechanisms of action may also contribute to this activity. In fact, the ability of these agents to produce ROS may lead to the inhibition of the NF-κB pathway, which is sensitive to ROS (Morgan and Liu, 2011). Importantly, the multi-faceted effect of these agents is likely to make them superior to classical single-targeted inhibitors of the NF-κB pathway.

In conclusion, we demonstrate herein that the metastasis suppressor, NDRG1, inhibits the expression of the oncogenic LYRIC *via* its ability to inhibit the PI3K/AKT pathway. Further, a novel class of anti-cancer agents that up-regulate NDRG1 were also found to inhibit LYRIC expression and its participation in the oncogenic NF-κB signaling pathway. These results further highlight the marked potential of DpC and its ability to target LYRIC, another vital player in oncogenesis.

Molecular Pharmacology Fast Forward. Published on March 8, 2017 as DOI: 10.1124/mol.116.107870
This article has not been copyedited and formatted. The final version may differ from this version.

CONFLICT OF INTEREST: D.R.R. is a stakeholder in the companies, Oncochel Therapeutics LLC and Pty. Ltd, which are developing DpC for the treatment of advanced and resistant solid tumors.

AUTHORSHIP CONTRIBUTIONS:

Participated in research design: Zhang, Richardson, Kovacevic

Conducted experiments: Xi, Pun, Menezes, Fouani, Huang

Performed data analysis: Xi, Pun, Menezes, Huang, Kovacevic

Wrote or contributed to the writing of the manuscript: Xi, Pun, Kalinowski, Richardson, Kovacevic

Molecular Pharmacology Fast Forward. Published on March 8, 2017 as DOI: 10.1124/mol.116.107870
This article has not been copyedited and formatted. The final version may differ from this version.

REFERENCES:

Balkwill F (2009) Tumour necrosis factor and cancer. *Nat Rev Cancer* **9**: 361-371.

Bharti AC and BB Aggarwal (2002) Nuclear factor-kappa B and cancer: its role in prevention and therapy. *Biochemical Pharmacology* **64**: 883-888.

Chen Z, D Zhang, F Yue, M Zheng, Z Kovacevic and DR Richardson (2012) The iron chelators Dp44mT and DFO inhibit TGF-beta-induced epithelial-mesenchymal transition via up-regulation of N-Myc downstream-regulated gene 1 (NDRG1). *J Biol Chem* **287**: 17016-17028.

Dixon KM, GYL Lui, Z Kovacevic, D Zhang, M Yao, Z Chen, Q Dong, SJ Assinder and DR Richardson (2013) Dp44mT targets the AKT, TGF-β and ERK pathways via the metastasis suppressor NDRG1 in normal prostate epithelial cells and prostate cancer cells. *Br J Cancer* **108**: 409-419.

Ellen TP, Q Ke, P Zhang and M Costa (2008) NDRG1, a growth and cancer related gene: regulation of gene expression and function in normal and disease states. *Carcinogenesis* **29**: 2-8.

Emdad L, SK Das, S Dasgupta, B Hu, D Sarkar and PB Fisher (2013) AEG-1/MTDH/LYRIC: signaling pathways, downstream genes, interacting proteins, and regulation of tumor angiogenesis. *Adv Cancer Res* **120**: 75-111.

Emdad L, D Sarkar, ZZ Su, SG Lee, DC Kang, JN Bruce, DJ Volsky and PB Fisher (2007) Astrocyte elevated gene-1: recent insights into a novel gene involved in tumor progression, metastasis and neurodegeneration. *Pharmacol Ther* **114**: 155-170.

Emdad L, D Sarkar, ZZ Su, A Randolph, H Boukerche, K Valerie and PB Fisher (2006) Activation of the nuclear factor kappaB pathway by astrocyte elevated gene-1: implications for tumor progression and metastasis. *Cancer Res* **66**: 1509-1516.

Fang BA, Z Kovacevic, KC Park, DS Kalinowski, PJ Jansson, DJ Lane, S Sahni and DR Richardson (2014) Molecular functions of the iron-regulated metastasis suppressor, NDRG1, and its potential as a molecular target for cancer therapy. *Biochim Biophys Acta* **1845**: 1-19.

Flohe L, R Brigelius-Flohe, C Saliou, MG Traber and L Packer (1997) Redox regulation of NF-kappa B activation. *Free Radic Biol Med* **22**: 1115-1126.

Ghalayini MK, Q Dong, DR Richardson and SJ Assinder (2013) Proteolytic cleavage and truncation of NDRG1 in human prostate cancer cells, but not normal prostate epithelial cells. *Biosci Rep* **33**: 451-461.

Guo ZL, DR Richardson, DS Kalinowski, Z Kovacevic, KC Tan-Un and GC Chan (2016) The novel thiosemicarbazone, di-2-pyridylketone 4-cyclohexyl-4-methyl-3-thiosemicarbazone (DpC), inhibits neuroblastoma growth in vitro and in vivo via multiple mechanisms. *J Hematol Oncol* **9**: 98.

Ho MY, SJ Tang, MJ Chuang, TL Cha, JY Li, GH Sun and KH Sun (2012) TNF-alpha induces epithelial-mesenchymal transition of renal cell carcinoma cells via a GSK3beta-dependent mechanism. *Mol Cancer Res* **10**: 1109-1119.

Hosoi F, H Izumi, A Kawahara, Y Murakami, H Kinoshita, M Kage, K Nishio, K Kohno, M Kuwano and M Ono (2009) N-myc downstream regulated gene 1/Cap43 suppresses tumor growth and angiogenesis of pancreatic cancer through attenuation of inhibitor of kappaB kinase beta expression. *Cancer Res* **69**: 4983-4991.

Hussain AR, SO Ahmed, M Ahmed, OS Khan, S Al Abdulmohsen, LC Platanias, KS Al-Kuraya and S Uddin (2012) Cross-talk between NFkB and the PI3-kinase/AKT pathway can be targeted in primary effusion lymphoma (PEL) cell lines for efficient apoptosis. *PLoS One* **7**: e39945.

Jansson PJ, DS Kalinowski, DJ Lane, Z Kovacevic, NA Seebacher, L Fouani, S Sahni, AM Merlot and DR Richardson (2015) The renaissance of polypharmacology in the development of anti-cancer therapeutics: Inhibition of the "Triad of Death" in cancer by Di-2-pyridylketone thiosemicarbazones. *Pharmacol Res* **100**: 255-260.

Jin R, W Liu, S Menezes, F Yue, M Zheng, Z Kovacevic and DR Richardson (2014) The metastasis suppressor NDRG1 modulates the phosphorylation and nuclear translocation of beta-catenin through mechanisms involving FRAT1 and PAK4. *J Cell Sci* **127**: 3116-3130.

Kalinowski DS and DR Richardson (2005) The evolution of iron chelators for the treatment of iron overload disease and cancer. *Pharmacol Rev* **57**: 547-583.

Kalinowski DS, C Stefani, S Toyokuni, T Ganz, GJ Anderson, NV Subramaniam, D Trinder, JK Olynyk, A Chua, PJ Jansson, S Sahni, DJ Lane, AM Merlot, Z Kovacevic, ML Huang, CS Lee and DR Richardson (2016) Redox cycling metals: Pedaling their roles in metabolism and their use in the development of novel therapeutics. *Biochim Biophys Acta* **1863**: 727-748.

Kalluri R and RA Weinberg (2009) The basics of epithelial-mesenchymal transition. *J Clin Invest* **119**: 1420-1428.

Kang DC, ZZ Su, D Sarkar, L Emdad, DJ Volsky and PB Fisher (2005) Cloning and characterization of HIV-1-inducible astrocyte elevated gene-1, AEG-1. *Gene* **353**: 8-15.

Karin M (2006) Nuclear factor-kappaB in cancer development and progression. *Nature* **441**: 431-436.

Karin M and FR Greten (2005) NF-kappaB: linking inflammation and immunity to cancer development and progression. *Nat Rev Immunol* **5**: 749-759.

Khuda, II, N Koide, AS Noman, J Dagvadorj, G Tumurkhuu, Y Naiki, T Komatsu, T Yoshida and T Yokochi (2009) Astrocyte elevated gene-1 (AEG-1) is induced by

lipopolysaccharide as toll-like receptor 4 (TLR4) ligand and regulates TLR4 signalling. *Immunology* **128**: e700-706.

Kovacevic Z, S Chikhani, DB Lovejoy and DR Richardson (2011) Novel thiosemicarbazone iron chelators induce up-regulation and phosphorylation of the metastasis suppressor N-myc down-stream regulated gene 1: a new strategy for the treatment of pancreatic cancer. *Mol Pharmacol* **80**: 598-609.

Kovacevic Z, S Chikhani, GYL Lui, S Sivagurunathan and DR Richardson (2013) The Iron-Regulated Metastasis Suppressor NDRG1 Targets NEDD4L, PTEN and SMAD4 and Inhibits The PI3K and Ras Signaling Pathways. *Antioxidants and Redox Signalling* **18**: 874-887.

Kovacevic Z, D Fu and DR Richardson (2008) The iron-regulated metastasis suppressor, Ndrg-1: identification of novel molecular targets. *Biochim Biophys Acta* **1783**: 1981-1992.

Krishnan RK, H Nolte, T Sun, H Kaur, K Sreenivasan, M Looso, S Offermanns, M Kruger and JM Swiercz (2015) Quantitative analysis of the TNF-alpha-induced phosphoproteome reveals AEG-1/MTDH/LYRIC as an IKKbeta substrate. *Nat Commun* **6**: 6658.

Lane DJ, F Saletta, Y Suryo Rahmanto, Z Kovacevic and DR Richardson (2013) N-myc downstream regulated 1 (NDRG1) is regulated by eukaryotic initiation factor 3a (eIF3a) during cellular stress caused by iron depletion. *PLoS One* **8**: e57273.

Le NT and DR Richardson (2004) Iron chelators with high antiproliferative activity up-regulate the expression of a growth inhibitory and metastasis suppressor gene: a link between iron metabolism and proliferation. *Blood* **104**: 2967-2975.

Lee SG, ZZ Su, L Emdad, D Sarkar and PB Fisher (2006) Astrocyte elevated gene-1 (AEG-1) is a target gene of oncogenic Ha-ras requiring phosphatidylinositol 3-kinase and c-Myc. *Proc Natl Acad Sci U S A* **103**: 17390-17395.

Lee SG, ZZ Su, L Emdad, D Sarkar, TF Franke and PB Fisher (2008) Astrocyte elevated gene-1 activates cell survival pathways through PI3K-Akt signaling. *Oncogene* **27**: 1114-1121.

Li J, N Zhang, LB Song, WT Liao, LL Jiang, LY Gong, J Wu, J Yuan, HZ Zhang, MS Zeng and M Li (2008) Astrocyte elevated gene-1 is a novel prognostic marker for breast cancer progression and overall patient survival. *Clin Cancer Res* **14**: 3319-3326.

Li X, X Kong, Q Huo, H Guo, S Yan, C Yuan, MS Moran, C Shao and Q Yang (2011) Metadherin enhances the invasiveness of breast cancer cells by inducing epithelial to mesenchymal transition. *Cancer Sci* **102**: 1151-1157.

Liu P, H Cheng, TM Roberts and JJ Zhao (2009) Targeting the phosphoinositide 3-kinase pathway in cancer. *Nat Rev Drug Discov* **8**: 627-644.

Liu W, F Xing, M Iiizumi-Gairani, H Okuda, M Watabe, SK Pai, PR Pandey, S Hirota, A Kobayashi, YY Mo, K Fukuda, Y Li and K Watabe (2012) N-myc downstream regulated gene 1 modulates Wnt-beta-catenin signalling and pleiotropically suppresses metastasis. *EMBO Mol Med* **4**: 93-108.

Liu W, F Yue, M Zheng, A Merlot, DH Bae, M Huang, D Lane, P Jansson, GY Lui, V Richardson, S Sahni, D Kalinowski, Z Kovacevic and DR Richardson (2015) The proto-oncogene c-Src and its downstream signaling pathways are inhibited by the metastasis suppressor, NDRG1. *Oncotarget* **6**: 8851-8874.

Lovejoy DB, DM Sharp, N Seebacher, P Obeidy, T Prichard, C Stefani, MT Basha, PC Sharpe, PJ Jansson, DS Kalinowski, PV Bernhardt and DR Richardson (2012) Novel second-generation di-2-pyridylketone thiosemicarbazones show synergism with standard

chemotherapeutics and demonstrate potent activity against lung cancer xenografts after oral and intravenous administration in vivo. *J Med Chem* **55**: 7230-7244.

Mochizuki Y, H Nakanishi, Y Kodera, S Ito, Y Yamamura, T Kato, K Hibi, S Akiyama, A Nakao and M Tatematsu (2004) TNF-alpha promotes progression of peritoneal metastasis as demonstrated using a green fluorescence protein (GFP)-tagged human gastric cancer cell line. *Clin Exp Metastasis* **21**: 39-47.

Morgan MJ and ZG Liu (2011) Crosstalk of reactive oxygen species and NF-kappaB signaling. *Cell Res* **21**: 103-115.

Murakami Y, F Hosoi, H Izumi, Y Maruyama, H Ureshino, K Watari, K Kohno, M Kuwano and M Ono (2010) Identification of sites subjected to serine/threonine phosphorylation by SGK1 affecting N-myc downstream-regulated gene 1 (NDRG1)/Cap43-dependent suppression of angiogenic CXC chemokine expression in human pancreatic cancer cells. *Biochem Biophys Res Commun* **396**: 376-381.

Richardson DR, PC Sharpe, DB Lovejoy, D Senaratne, DS Kalinowski, M Islam and PV Bernhardt (2006) Dipyridyl thiosemicarbazone chelators with potent and selective antitumor activity form iron complexes with redox activity. *J Med Chem* **49**: 6510-6521.

Sarkar D and PB Fisher (2013) AEG-1/MTDH/LYRIC: clinical significance. *Adv Cancer Res* **120**: 39-74.

Sarkar D, ES Park, L Emdad, SG Lee, ZZ Su and PB Fisher (2008) Molecular basis of nuclear factor-kappaB activation by astrocyte elevated gene-1. *Cancer Res* **68**: 1478-1484.

Seebacher NA, DJ Lane, PJ Jansson and DR Richardson (2016) Glucose modulation induces lysosome formation and increases lysosomotropic drug sequestration via the p-glycoprotein drug transporter. *J Biol Chem* **291**: 3796-3820.

Seebacher NA, DR Richardson and PJ Jansson (2016) A mechanism for overcoming P-glycoprotein-mediated drug resistance: novel combination therapy that releases stored

doxorubicin from lysosomes via lysosomal permeabilization using Dp44mT or DpC. *Cell Death Dis* **7**: e2510.

Shah MA, N Kemeny, A Hummer, M Drobnjak, M Motwani, C Cordon-Cardo, M Gonen and GK Schwartz (2005) Drg1 expression in 131 colorectal liver metastases: correlation with clinical variables and patient outcomes. *Clin Cancer Res* **11**: 3296-3302.

Shi X and X Wang (2015) The role of MTDH/AEG-1 in the progression of cancer. *Int J Clin Exp Med* **8**: 4795-4807.

Stacy AE, D Palanimuthu, PV Bernhardt, DS Kalinowski, PJ Jansson and DR Richardson (2016) Structure-activity relationships of di-2-pyridylketone, 2-benzoylpyridine, and 2-acetylpyridine thiosemicarbazones for overcoming pgp-mediated drug resistance. *J Med Chem* **59**: 8601-8620.

Su ZZ, Y Chen, DC Kang, W Chao, M Simm, DJ Volsky and PB Fisher (2003) Customized rapid subtraction hybridization (RaSH) gene microarrays identify overlapping expression changes in human fetal astrocytes resulting from human immunodeficiency virus-1 infection or tumor necrosis factor-alpha treatment. *Gene* **306**: 67-78.

Su ZZ, DC Kang, Y Chen, O Pekarskaya, W Chao, DJ Volsky and PB Fisher (2002) Identification and cloning of human astrocyte genes displaying elevated expression after infection with HIV-1 or exposure to HIV-1 envelope glycoprotein by rapid subtraction hybridization, RaSH. *Oncogene* **21**: 3592-3602.

Sun J, D Zhang, Y Zheng, Q Zhao, M Zheng, Z Kovacevic and DR Richardson (2013) Targeting the metastasis suppressor, NDRG1, using novel iron chelators: regulation of stress fiber-mediated tumor cell migration via modulation of the ROCK1/pMLC2 signaling pathway. *Mol Pharmacol* **83**: 454-469.

Wan L, X Lu, S Yuan, Y Wei, F Guo, M Shen, M Yuan, R Chakrabarti, Y Hua, HA Smith, MA Blanco, M Chekmareva, H Wu, RT Bronson, BG Haffty, Y Xing and Y Kang

(2014) MTDH-SND1 interaction is crucial for expansion and activity of tumor-initiating cells in diverse oncogene- and carcinogen-induced mammary tumors. *Cancer Cell* **26**: 92-105.

Wang X and Y Lin (2008) Tumor necrosis factor and cancer, buddies or foes? *Acta Pharmacol Sin* **29**: 1275-1288.

Wang Z, ZY Tang, Z Yin, YB Wei, LF Liu, B Yan, KQ Zhou, YQ Nian, YL Gao and JR Yang (2016) Metadherin regulates epithelial-mesenchymal transition in carcinoma. *Onco Targets Ther* **9**: 2429-2436.

Wangpu X, J Lu, R Xi, F Yue, S Sahni, KC Park, S Menezes, ML Huang, M Zheng, Z Kovacevic and DR Richardson (2016) Targeting the metastasis suppressor, N-myc downstream regulated gene-1, with novel di-2-pyridylketone thiosemicarbazones: Suppression of tumor cell migration and cell-collagen adhesion by inhibiting focal adhesion kinase/paxillin signaling. *Mol Pharmacol* **89**: 521-540.

Wangpu X, X Yang, J Zhao, J Lu, S Guan, J Lu, Z Kovacevic, W Liu, L Mi, R Jin, J Sun, F Yue, J Ma, A Lu, DR Richardson, L Wang and M Zheng (2015) The metastasis suppressor, NDRG1, inhibits "stemness" of colorectal cancer via down-regulation of nuclear beta-catenin and CD44. *Oncotarget* **6**: 33893-33911.

Whitnall M, J Howard, P Ponka and DR Richardson (2006) A class of iron chelators with a wide spectrum of potent antitumor activity that overcomes resistance to chemotherapeutics. *Proc Natl Acad Sci U S A* **103**: 14901-14906.

Wu Y, J Deng, PG Rychahou, SM Qiu, BM Evers and BPH Zhou (2009) Stabilization of Snail by NF-kappa B Is Required for Inflammation-Induced Cell Migration and Invasion. *Cancer Cell* **15**: 416-428.

Yoo BK, L Emdad, ZZ Su, A Villanueva, DY Chiang, ND Mukhopadhyay, AS Mills, S Waxman, RA Fisher, JM Llovet, PB Fisher and D Sarkar (2009) Astrocyte elevated gene-1 regulates hepatocellular carcinoma development and progression. *J Clin Invest* **119**: 465-477.

Yuan J, DB Lovejoy and DR Richardson (2004) Novel di-2-pyridyl-derived iron chelators with marked and selective antitumor activity: in vitro and in vivo assessment. *Blood* **104**: 1450-1458.

Zhang J, S Chen, W Zhang, J Zhang, X Liu, H Shi, H Che, W Wang, F Li and L Yao (2008) Human differentiation-related gene NDRG1 is a Myc downstream-regulated gene that is repressed by Myc on the core promoter region. *Gene* **417**: 5-12.

Zhu J, J Blenis and J Yuan (2008) Activation of PI3K/Akt and MAPK pathways regulates Myc-mediated transcription by phosphorylating and promoting the degradation of Mad1. *Proc Natl Acad Sci U S A* **105**: 6584-6589.

FOOTNOTES:

R.X. and I.H.Y.P. contributed equally to this manuscript. D.R.R. and Z.K. are co-corresponding authors. This work was supported by a scholarship from The National Natural Science Foundation of China [NO.81272775]; a Student Attachment Program Scholarship from the Hong Kong Polytechnic University; Australian Postgraduate Awards from the University of Sydney; a Senior Principal Research Fellowship [1062607], Peter Doherty Early Career Fellowships [1037323, 1074033], a RD Wright Career Development Fellowship [1083057] and Project Grants from the National Health and Medical Research Council of Australia [1060482]; Cancer Australia and Cure Cancer Australia priority driven collaborative cancer research scheme [1086449]; and a Cancer Institute New South Wales Early Career Fellowship [12-ECF2-17].

Molecular Pharmacology Fast Forward. Published on March 8, 2017 as DOI: 10.1124/mol.116.107870
This article has not been copyedited and formatted. The final version may differ from this version.

FIGURE LEGENDS

Figure 1. (**A**) **Line drawings of the chemical structures of DpC, Dp44mT, DFO and Bp2mT and NDRG1 inhibits LYRIC expression in (B) DU145 and (C) HT29 cells.** The expression of NDRG1 and LYRIC was examined in (**B**) DU145 and (**C**) HT29 cells stably transfected to over-express NDRG1 (NDRG1) or the relevant empty Vector Ctrl, as well as cells stably transfected with *NDRG1* shRNA to silence this protein (sh-NDRG) or the relevant control shRNA (sh-Ctrl). Immunoblots shown are representative of at least three independent experiments. Densitometry data are expressed relative to β-actin and shown as mean ± S.D. (3-5 experiments). Relative to the respective Vector Ctrl or sh-Ctrl cells, as appropriate: $^{**}p < 0.01$, $^{***}p < 0.001$.

Figure 2. Up-regulation of NDRG1 attenuates the TNFα-induced expression of LYRIC and characteristics of the EMT. (**A**) DU145 and (**B**) HT29 Vector Ctrl, NDRG1, sh-Ctrl and sh-NDRG1 cells were incubated with or without TNFα (20 ng/mL; 48 h/37ºC) and Western blotting conducted to detect the expression of NDRG1, LYRIC, NF-κB p65 and vimentin. Immunoblots shown are representative of 3 independent experiments. Densitometry data are expressed relative to β-actin and shown as mean ± S.D. (3-5 experiments). Relative to the respective TNFα untreated control: $^{*}p < 0.05$, $^{**}p < 0.01$, $^{***}p < 0.001$. Relative to the relevant Vector Ctrl or sh-Ctrl: $\dagger\dagger\dagger p < 0.001$. **(C)** Transwell migration assays with DU145 and HT29 Vector Ctrl and NDRG1 over-expressing cells, or **(D)** sh-Ctrl and sh-NDRG1 cells in the presence of absence of TNFα (20 ng/mL; 48 h/37ºC). Representative images of cell migratory activity in transwell chambers are shown after 12 h/37ºC (DU145), or 36 h/37ºC (HT29). The number of migrating cells was quantified by direct counting of stained cells, with 5 random fields used for each sample, and is presented

Molecular Pharmacology Fast Forward. Published on March 8, 2017 as DOI: 10.1124/mol.116.107870
This article has not been copyedited and formatted. The final version may differ from this version.

as mean ± S.D. Relative to Vector Ctrl or sh-Ctrl without TNFα: ***$p < 0.001$. Relative to Vector Ctrl or sh-Ctrl with TNFα: ††$p < 0.01$, †††$p < 0.001$.

Figure 3. The iron chelator DFO and thiosemicarbazones, DpC and Dp44mT, decrease the expression of LYRIC, while up-regulating NDRG1 in DU145 and HT29 cells. DU145 and HT29 cells were incubated with either Bp2mT (10 μM), DFO (250 μM), Dp44mT (10 μM), or DpC (10 μM), for 24 h/37ºC and assessed for *NDRG1* and *LYRIC* expression at the mRNA level *via* RT-PCR (**A**, **B**), qRT-PCR (**C**, **D**), or at the protein level using western blotting (**E**, **F**). Densitometry data are expressed relative to β-actin and shown as mean ± S.D. (3-5 experiments). Relative to the respective untreated control cells **$p < 0.01$, ***$p < 0.001$.

Figure 4. The thiosemicarbazones, DpC and Dp44mT, attenuate the TNFα-induced expression of LYRIC, NF-κB p65 and vimentin in DU145 and HT29 cells. (**A**) DU145 and (**B**) HT29 cells were incubated with or without TNFα (20 ng/mL; 48 h/37ºC) and treated with either: Bp2mT (10 μM), DFO (250 μM), Dp44mT (10 μM), or DpC (10 μM), for the last 24 h/37ºC. The expression of NDRG1, LYRIC, NF-κB p65 and vimentin expression was detected *via* Western blotting. Densitometry data are expressed relative to β-actin and shown as mean ± S.D. (3-5 experiments). Relative to the untreated control cells: *$p < 0.05$, **$p < 0.01$, ***$p < 0.001$.

Figure 5. The iron chelator DFO and thiosemicarbazones, DpC and Dp44mT, reduce the co-localization of LYRIC with NF-κB p65 as well as the translocation of NF-κB p65 into the nucleus in DU145 cells. DU145 cells were incubated without (**A**) or with (**B**) TNFα

Molecular Pharmacology Fast Forward. Published on March 8, 2017 as DOI: 10.1124/mol.116.107870
This article has not been copyedited and formatted. The final version may differ from this version.

(20 ng/mL; 48 h/37ºC) and treated with either: Bp2mT (10 μM), DFO (250 μM), Dp44mT (10 μM), or DpC (10 μM), for the last 24 h/37ºC. The localization of LYRIC and NF-κB p65 was examined *via* immunofluorescence (as described in the *Materials and Methods*). The Mander's overlap coefficient was used to assess NF-κB p65 co-localization with the nucleus (DAPI) and was calculated for the enlarged sections of each merged image (as shown by white rectangles) using ImageJ software. The co-localization intensity of LYRIC with NF-κB p65 (**C**) and NF-κB p65 with the nucleus (DAPI; **D**) was quantified using ImageJ software. The scale bar in the bottom right corner of the first image represents 50 μm and is the same across all unmagnified images. Relative to the untreated control cells: $*p < 0.05$, $**p < 0.01$, $***p < 0.001$.

Figure 6. The iron chelator DFO and thiosemicarbazones, DpC and Dp44mT, reduce the co-localization of LYRIC with NF-κB p65 as well as the translocation of NF-κB p65 into the nucleus in HT29 cells. HT29 cells were incubated without (**A**) or with (**B**) TNFα (20 ng/mL; 48 h/37ºC) and treated with either: Bp2mT (10 μM), DFO (250 μM), Dp44mT (10 μM), or DpC (10 μM), for the last 24 h/37ºC. The localization of LYRIC and NF-κB p65 was examined *via* immunofluorescence (as described in the *Materials and Methods*). The Mander's overlap coefficient was used to assess NF-κB p65 co-localization with the nucleus (DAPI) and was calculated for the enlarged sections of each merged image (as shown by white rectangles) using ImageJ software. The co-localization intensity of LYRIC with NF-κB p65 (**C**) and NF-κB p65 with the nucleus (DAPI; **D**) was quantified using the ImageJ software. The scale bar in the bottom right corner of the first image represents 50 μm and is the same across all unmagnified images. Relative to the untreated control cells: $**p < 0.01$, $***p < 0.001$.

Molecular Pharmacology Fast Forward. Published on March 8, 2017 as DOI: 10.1124/mol.116.107870
This article has not been copyedited and formatted. The final version may differ from this version.

Figure 7. The iron chelator, DFO, and thiosemicarbazones, DpC and Dp44mT, inhibit LYRIC expression, at least in part, *via* their effects on NDRG1. NDRG1 and LYRIC negatively regulate each other. (**A**) DU145 and (**B**) HT29 sh-Ctrl and sh-NDRG1 cells were treated with either: Bp2mT (10 μM), DFO (250 μM), Dp44mT (10 μM), or DpC (10 μM), for 24 h/37ºC and the expression of NDRG1 and LYRIC examined *via* Western blotting. Densitometry data are expressed relative to β-actin and shown as mean ± S.D. (3-5 experiments). Relative to the untreated control cells: *$p < 0.05$, **$p < 0.01$, ***$p < 0.001$. Relative to the corresponding sh-Ctrl cells: †$p < 0.05$, ††$p < 0.01$, †††$p < 0.001$. DU145 (**C**) and HT29 (**D**) sh-Ctrl and sh-NDRG1 cells were treated with either control siRNA (si-Ctrl) or siRNA specific for *LYRIC* (si-LYRIC) and the expression of NDRG1 and LYRIC assessed *via* Western blotting. Densitometry data are expressed relative to β-actin and shown as mean ± S.D. (3-5 experiments). Relative to the corresponding si-Ctrl cells: **$p < 0.01$, ***$p < 0.001$. Relative to the corresponding sh-Ctrl cells: †$p < 0.05$.

Figure 8. NDRG1 expression modulates the PI3K pathway and c-Myc in DU145 cells. (**A**) DU145 Vector Ctrl and NDRG1 over-expressing cells or (**B**) sh-Ctrl and sh-NDRG1 cells were treated with or without TNFα (20 ng/mL; 48 h/37ºC) and assessed for the expression of PI3K pathway molecules, namely PI3K-p85, p-AKT, AKT, c-Myc and PTEN *via* Western blotting. Densitometry data are expressed relative to β-actin and shown as mean ± S.D. (3-5 experiments). Relative to untreated Vector Ctrl or sh-Ctrl cells, as appropriate: *$p < 0.05$, **$p < 0.01$, ***$p < 0.001$. Relative to the TNFα-treated Vector Ctrl or sh-Ctrl cells, as appropriate: †$p < 0.05$.

Molecular Pharmacology Fast Forward. Published on March 8, 2017 as DOI: 10.1124/mol.116.107870
This article has not been copyedited and formatted. The final version may differ from this version.

Figure 9. NDRG1 expression modulates the PI3K pathway and c-Myc in HT29 cells. (**A**) HT29 Vector Ctrl and NDRG1 over-expressing cells or (**B**) sh-Ctrl and sh-NDRG1 cells were treated with or without TNFα (20 ng/mL; 48 h/37ºC) and assessed for the expression of PI3K pathway molecules, namely PI3K-p85, pAKT, AKT, c-Myc and PTEN *via* Western blotting. Densitometry data are expressed relative to β-actin and shown as mean ± S.D. (3-5 experiments). Relative to untreated Vector Ctrl or sh-Ctrl cells, as appropriate: *$p < 0.05$, **$p < 0.01$, ***$p < 0.001$. Relative to TNFα treated Vector Ctrl or sh-Ctrl cells, as appropriate: †$p < 0.05$, †††$p < 0.001$ (**C**) DU145 sh-Ctrl and sh-NDRG1 cells were transiently transfected with *c-Myc* siRNA and assessed for the expression of NDRG1, c-Myc and LYRIC *via* Western blotting. Densitometry data are expressed relative to β-actin and shown as mean ± S.D. (3-5 experiments). Relative to sh-Ctrl cells: *$p < 0.05$, **$p < 0.01$. Relative to si-Ctrl treated cells under the same conditions: †$p < 0.05$.

Figure 10. DFO, DpC and Dp44mT have an inhibitory effect on the PI3K pathway and c-Myc. (**A**) DU145 and (**B**) HT29 cells were treated with either: Bp2mT (10 μM), DFO (250 μM), Dp44mT (10 μM), or DpC (10 μM), for 24 h/37ºC and the expression of PI3K pathway molecules, namely PI3K-p85, p-AKT, AKT, c-Myc and PTEN was assessed *via* Western blotting. Densitometry data are expressed relative to β-actin and shown as mean ± S.D. (3-5 experiments). Relative to the untreated control cells: *$p < 0.05$, **$p < 0.01$, ***$p < 0.001$.

Figure 11. Schematic diagram of the interaction between NDRG1 with LYRIC and the molecular pathways involved. TNFα stimulates the PI3K and NF-κB signaling pathways by binding to the TNFα receptor (TNFR) (Su et al., 2002, Su et al., 2003). The PI3K pathway, *via* the activation of AKT enables c-Myc to promote the transcriptional up-regulation of

Molecular Pharmacology Fast Forward. Published on March 8, 2017 as DOI: 10.1124/mol.116.107870
This article has not been copyedited and formatted. The final version may differ from this version.

LYRIC (Lee et al., 2006). Concurrently, IKK is also able to phosphorylate LYRIC, promoting its activity (Krishnan et al., 2015). LYRIC is then able to: (***i***) reduce the expression of the inhibitory IκB subunit, releasing the active NF-κB p65/p50 complex, and; (***ii***) bind to the NF-κB p65 subunit and translocate into the nucleus where it promotes the expression of genes that regulate cell proliferation, invasion, *etc* (Emdad et al., 2006, Sarkar et al., 2008). The current study demonstrates that the metastasis suppressor, NDRG1, has an inhibitory effect on the PI3K pathway, reducing the levels of PI3K (p85 subunit), AKT and c-Myc, leading to reduced LYRIC levels. Interestingly, LYRIC itself also exerts an inhibitory effect on NDRG1. NDRG1 also promotes the expression of PTEN, an inhibitor of the PI3K pathway. The iron chelator, DFO, or novel thiosemicarbazones, DpC and Dp44mT, have similar inhibitory effects on LYRIC and the PI3K pathway and this is mediated, at least in part, *via* their ability to up-regulate NDRG1.

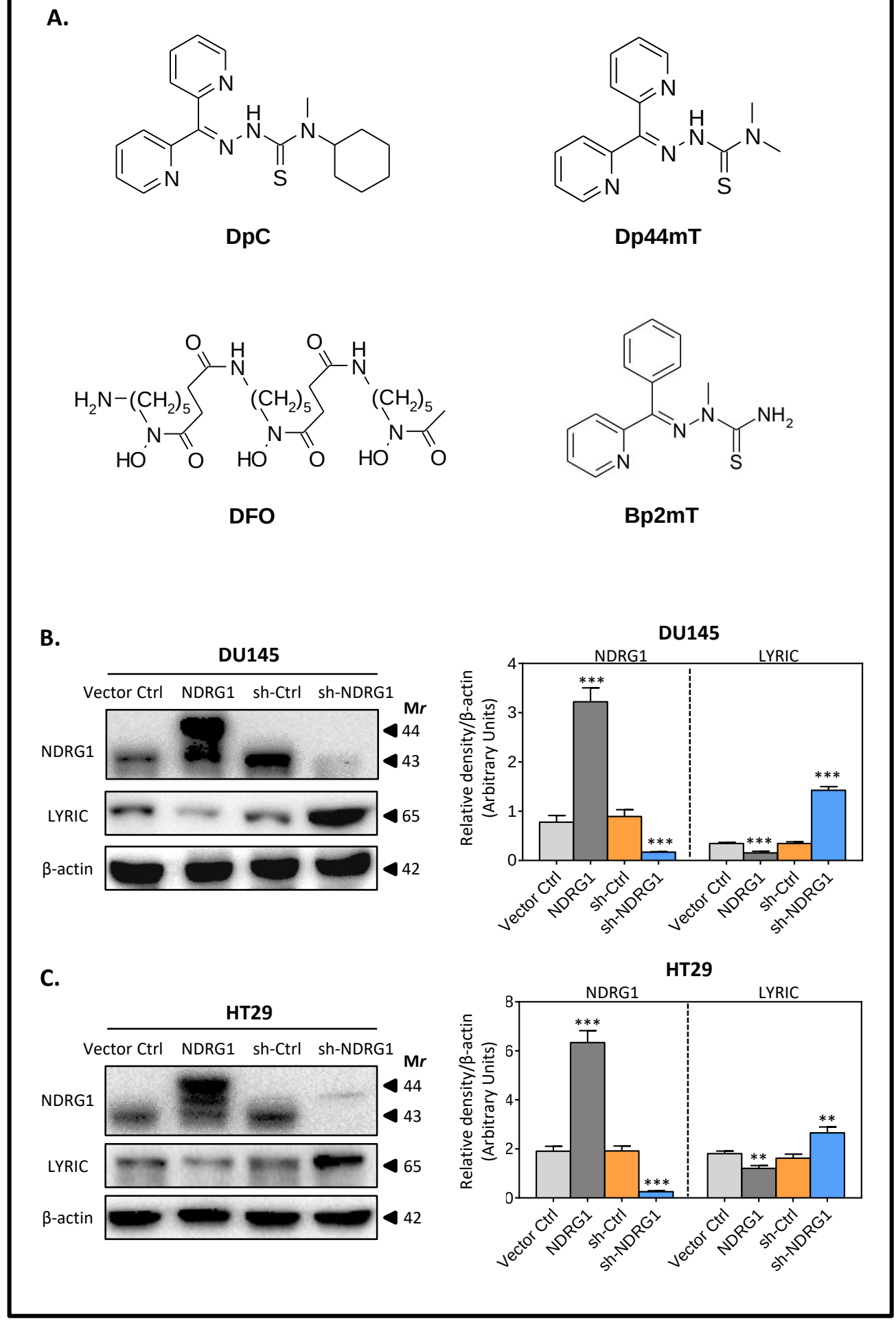
A.
DpC
Dp44mT
DFO
Bp2mT
B.
DU145
Vector Ctrl
NDRG1
sh-Ctrl
sh-NDRG1
Mr
NDRG1
LYRIC
β-actin
44
43
65
42
DU145
NDRG1
LYRIC
Relative density/β-actin (Arbitrary Units)
Vector Ctrl
NDRG1
sh-Ctrl
sh-NDRG1
C.
HT29
HT29

Figure 1

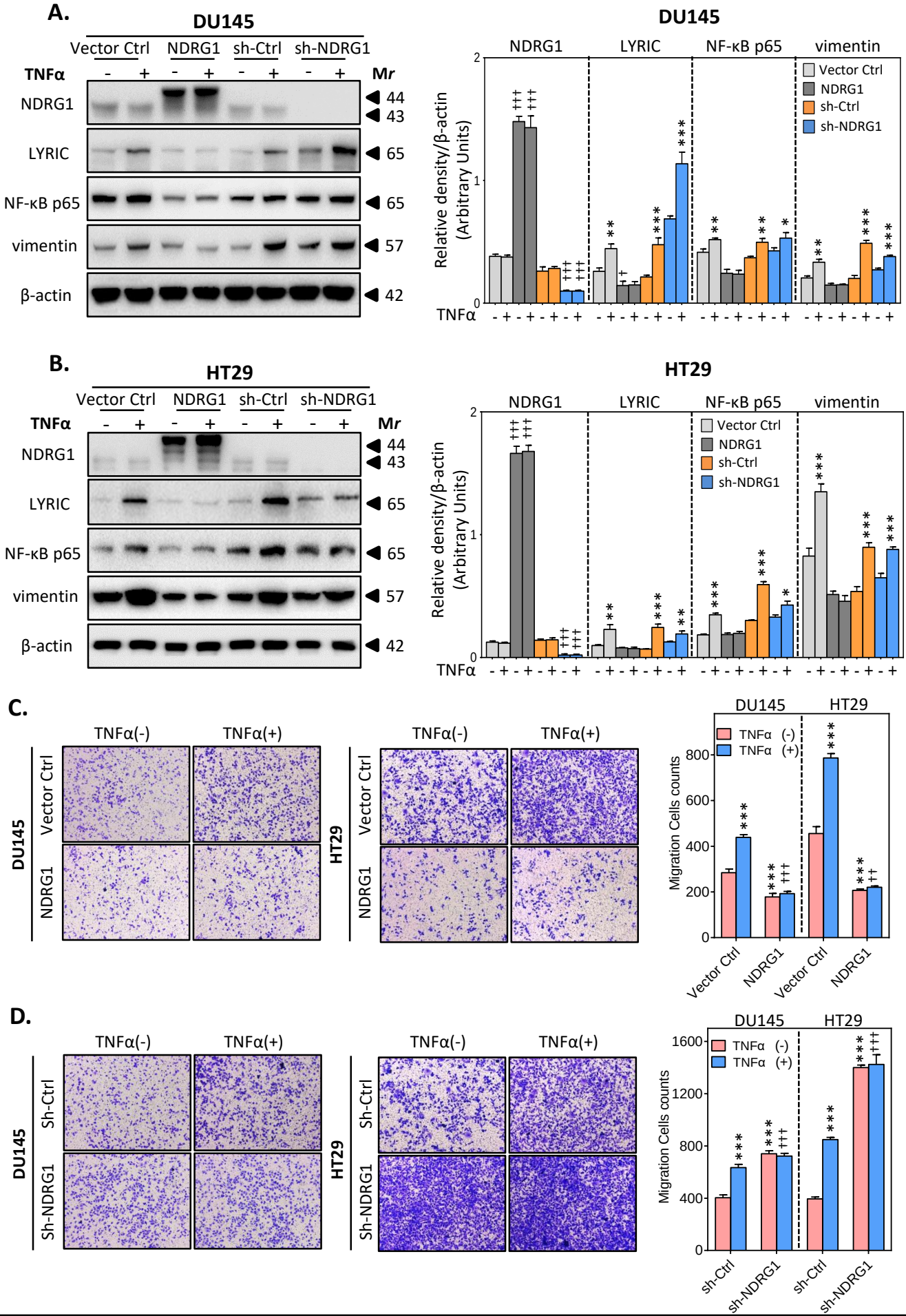
A.
DU145
Vector Ctrl
NDRG1
sh-Ctrl
sh-NDRG1
TNFα
Mr
NDRG1
LYRIC
NF-κB p65
vimentin
β-actin
44
43
65
65
57
42
DU145
NDRG1
LYRIC
NF-κB p65
vimentin
Relative density/β-actin (Arbitrary Units)
Vector Ctrl
NDRG1
sh-Ctrl
sh-NDRG1
B.
HT29
HT29
C.
TNFα(-)
TNFα(+)
DU145
HT29
Migration Cells counts
TNFα (-)
TNFα (+)
D.
Sh-Ctrl
Sh-NDRG1

Figure 2

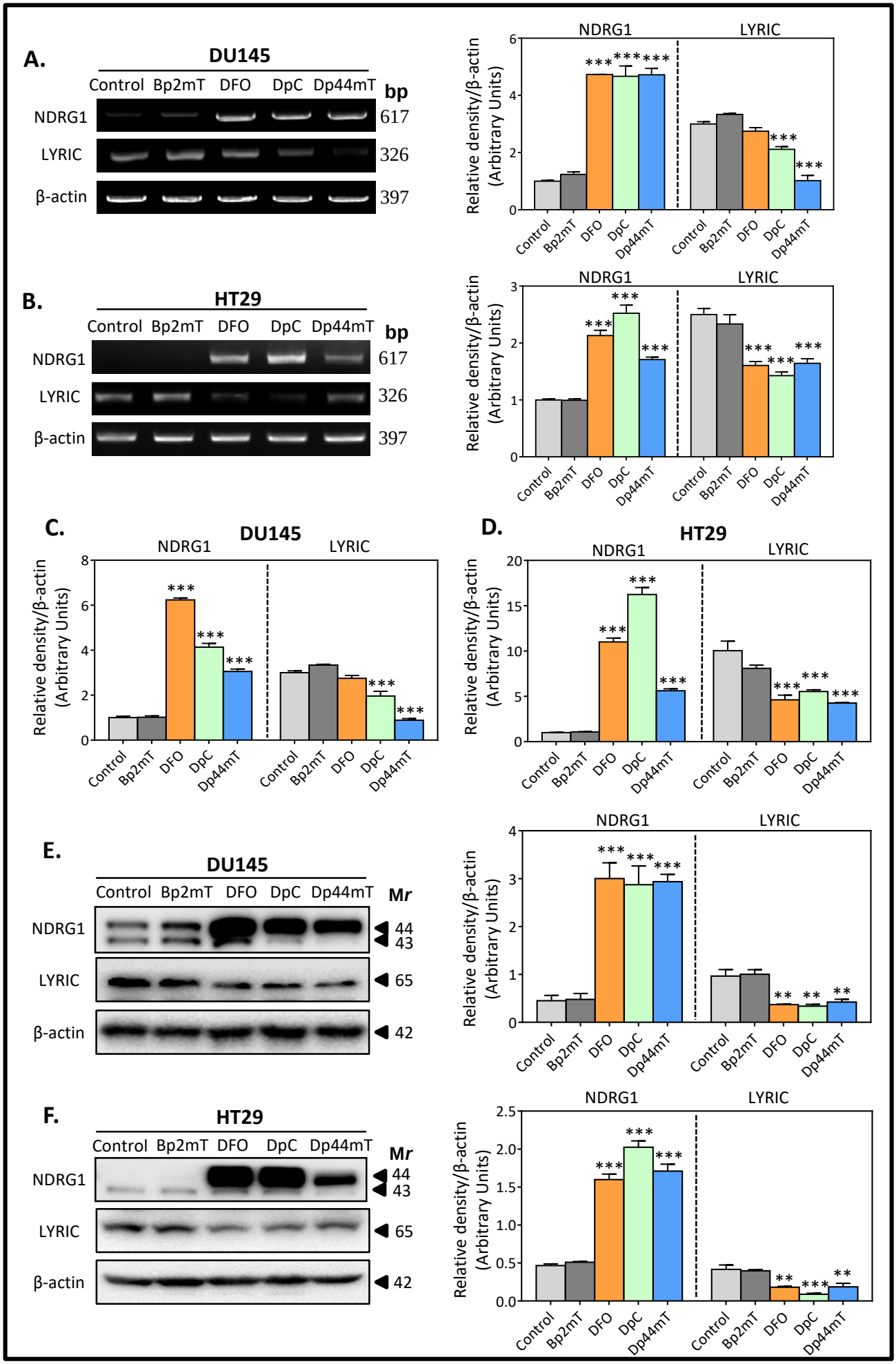
A.
DU145
Control Bp2mT DFO DpC Dp44mT
bp
NDRG1
LYRIC
β-actin
617
326
397
NDRG1
LYRIC
Relative density/β-actin (Arbitrary Units)
Control Bp2mT DFO DpC Dp44mT
B.
HT29
C.
D.
E.
Mr
44
43
65
42
F.

Figure 3

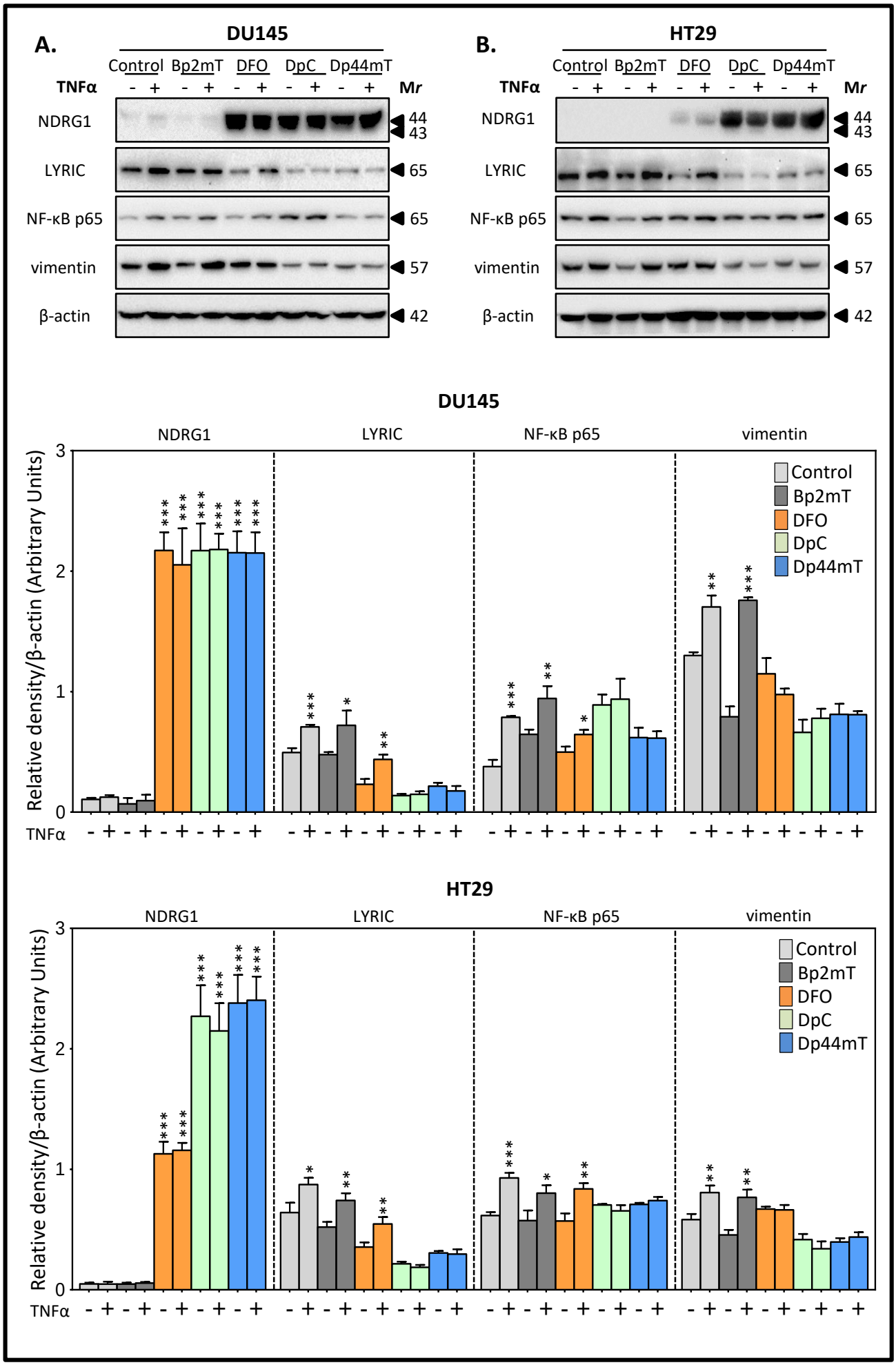
A.
DU145
Control Bp2mT DFO DpC Dp44mT
TNFα - + - + - + - + - + Mr
NDRG1 44 43
LYRIC 65
NF-κB p65 65
vimentin 57
β-actin 42
B.
HT29
Control Bp2mT DFO DpC Dp44mT
TNFα - + - + - + - + - + Mr
NDRG1 44 43
LYRIC 65
NF-κB p65 65
vimentin 57
β-actin 42
DU145
NDRG1
LYRIC
NF-κB p65
vimentin
Relative density/β-actin (Arbitrary Units)
Control
Bp2mT
DFO
DpC
Dp44mT
TNFα
HT29
NDRG1
LYRIC
NF-κB p65
vimentin
Relative density/β-actin (Arbitrary Units)
Control
Bp2mT
DFO
DpC
Dp44mT
TNFα

Figure 4

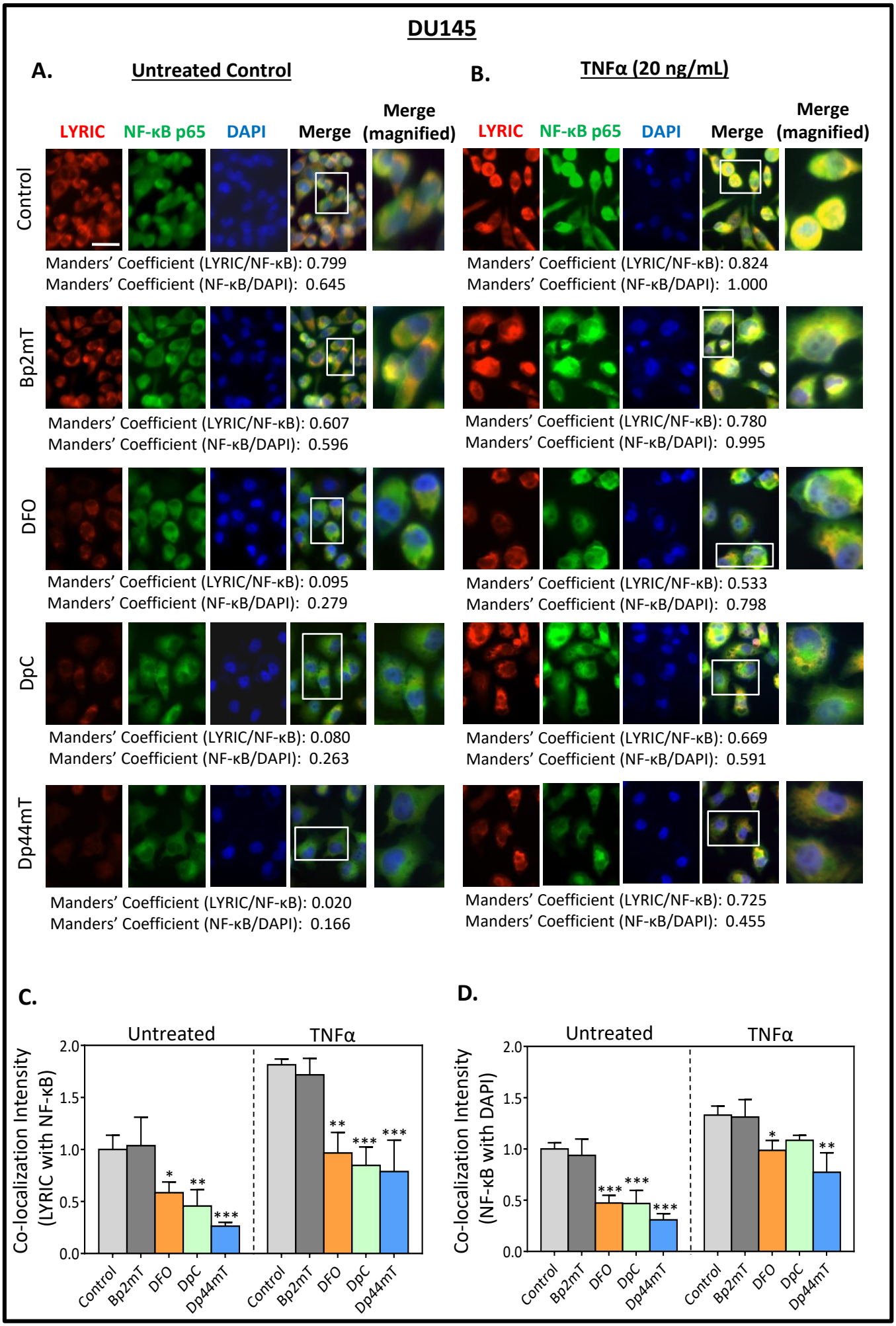
DU145
A.
Untreated Control
B.
TNFα (20 ng/mL)
LYRIC
NF-κB p65
DAPI
Merge
Merge (magnified)
Control
Manders' Coefficient (LYRIC/NF-κB): 0.799
Manders' Coefficient (NF-κB/DAPI): 0.645
Manders' Coefficient (LYRIC/NF-κB): 0.824
Manders' Coefficient (NF-κB/DAPI): 1.000
Bp2mT
Manders' Coefficient (LYRIC/NF-κB): 0.607
Manders' Coefficient (NF-κB/DAPI): 0.596
Manders' Coefficient (LYRIC/NF-κB): 0.780
Manders' Coefficient (NF-κB/DAPI): 0.995
DFO
Manders' Coefficient (LYRIC/NF-κB): 0.095
Manders' Coefficient (NF-κB/DAPI): 0.279
Manders' Coefficient (LYRIC/NF-κB): 0.533
Manders' Coefficient (NF-κB/DAPI): 0.798
DpC
Manders' Coefficient (LYRIC/NF-κB): 0.080
Manders' Coefficient (NF-κB/DAPI): 0.263
Manders' Coefficient (LYRIC/NF-κB): 0.669
Manders' Coefficient (NF-κB/DAPI): 0.591
Dp44mT
Manders' Coefficient (LYRIC/NF-κB): 0.020
Manders' Coefficient (NF-κB/DAPI): 0.166
Manders' Coefficient (LYRIC/NF-κB): 0.725
Manders' Coefficient (NF-κB/DAPI): 0.455
C.
Untreated
TNFα
Co-localization Intensity (LYRIC with NF-κB)
2.0
1.5
1.0
0.5
0.0
*
**
***
Control
Bp2mT
DFO
DpC
Dp44mT
D.
Co-localization Intensity (NF-κB with DAPI)

Figure 5

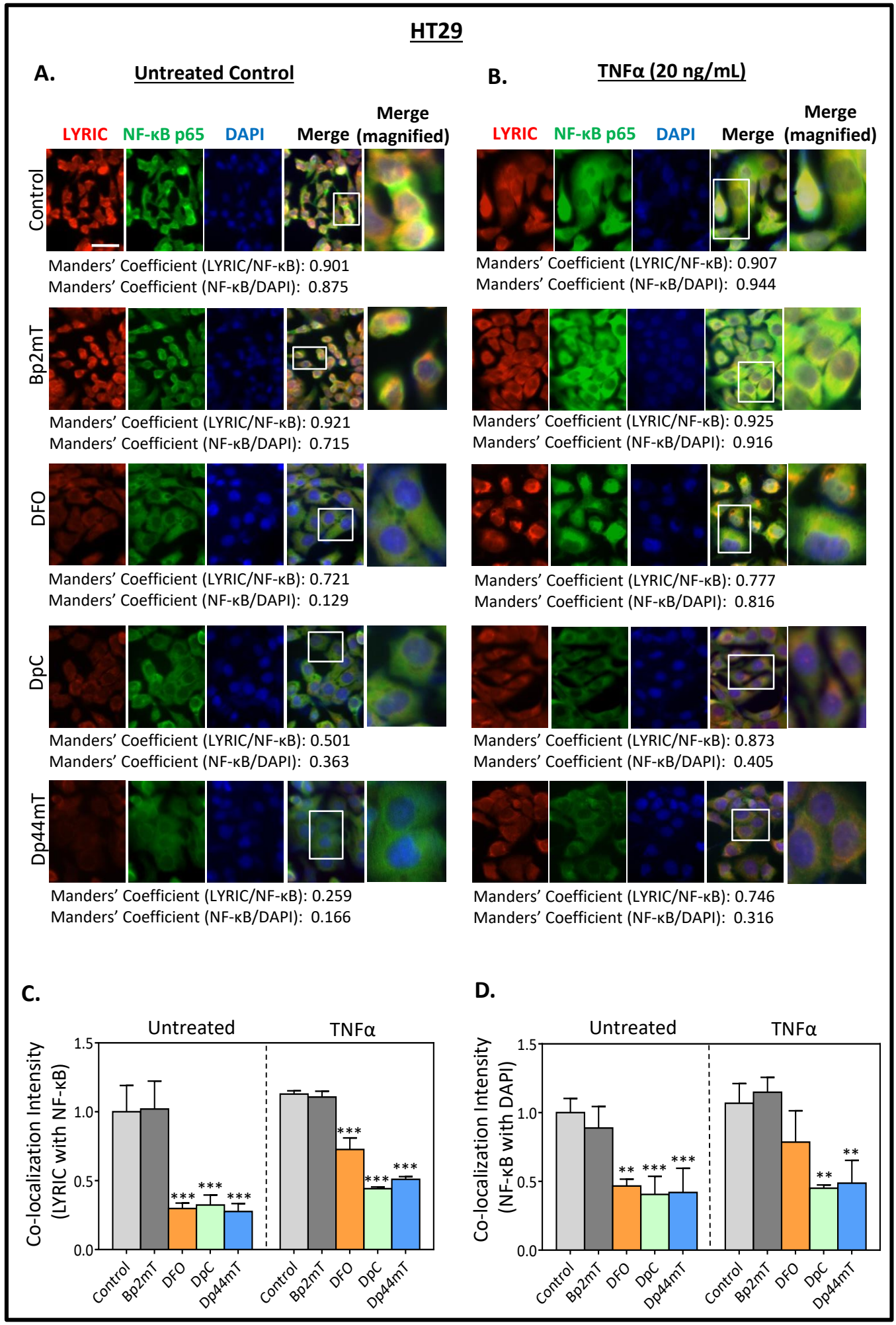
HT29
A.
Untreated Control
B.
TNFα (20 ng/mL)
LYRIC
NF-κB p65
DAPI
Merge
Merge (magnified)
Control
Bp2mT
DFO
DpC
Dp44mT
Manders' Coefficient (LYRIC/NF-κB): 0.901
Manders' Coefficient (NF-κB/DAPI): 0.875
Manders' Coefficient (LYRIC/NF-κB): 0.907
Manders' Coefficient (NF-κB/DAPI): 0.944
Manders' Coefficient (LYRIC/NF-κB): 0.921
Manders' Coefficient (NF-κB/DAPI): 0.715
Manders' Coefficient (LYRIC/NF-κB): 0.925
Manders' Coefficient (NF-κB/DAPI): 0.916
Manders' Coefficient (LYRIC/NF-κB): 0.721
Manders' Coefficient (NF-κB/DAPI): 0.129
Manders' Coefficient (LYRIC/NF-κB): 0.777
Manders' Coefficient (NF-κB/DAPI): 0.816
Manders' Coefficient (LYRIC/NF-κB): 0.501
Manders' Coefficient (NF-κB/DAPI): 0.363
Manders' Coefficient (LYRIC/NF-κB): 0.873
Manders' Coefficient (NF-κB/DAPI): 0.405
Manders' Coefficient (LYRIC/NF-κB): 0.259
Manders' Coefficient (NF-κB/DAPI): 0.166
Manders' Coefficient (LYRIC/NF-κB): 0.746
Manders' Coefficient (NF-κB/DAPI): 0.316
C.
Untreated
TNFα
Co-localization Intensity (LYRIC with NF-κB)
1.5
1.0
0.5
0.0
***
Control
Bp2mT
DFO
DpC
Dp44mT
D.
Untreated
TNFα
Co-localization Intensity (NF-κB with DAPI)
**
***

Figure 6

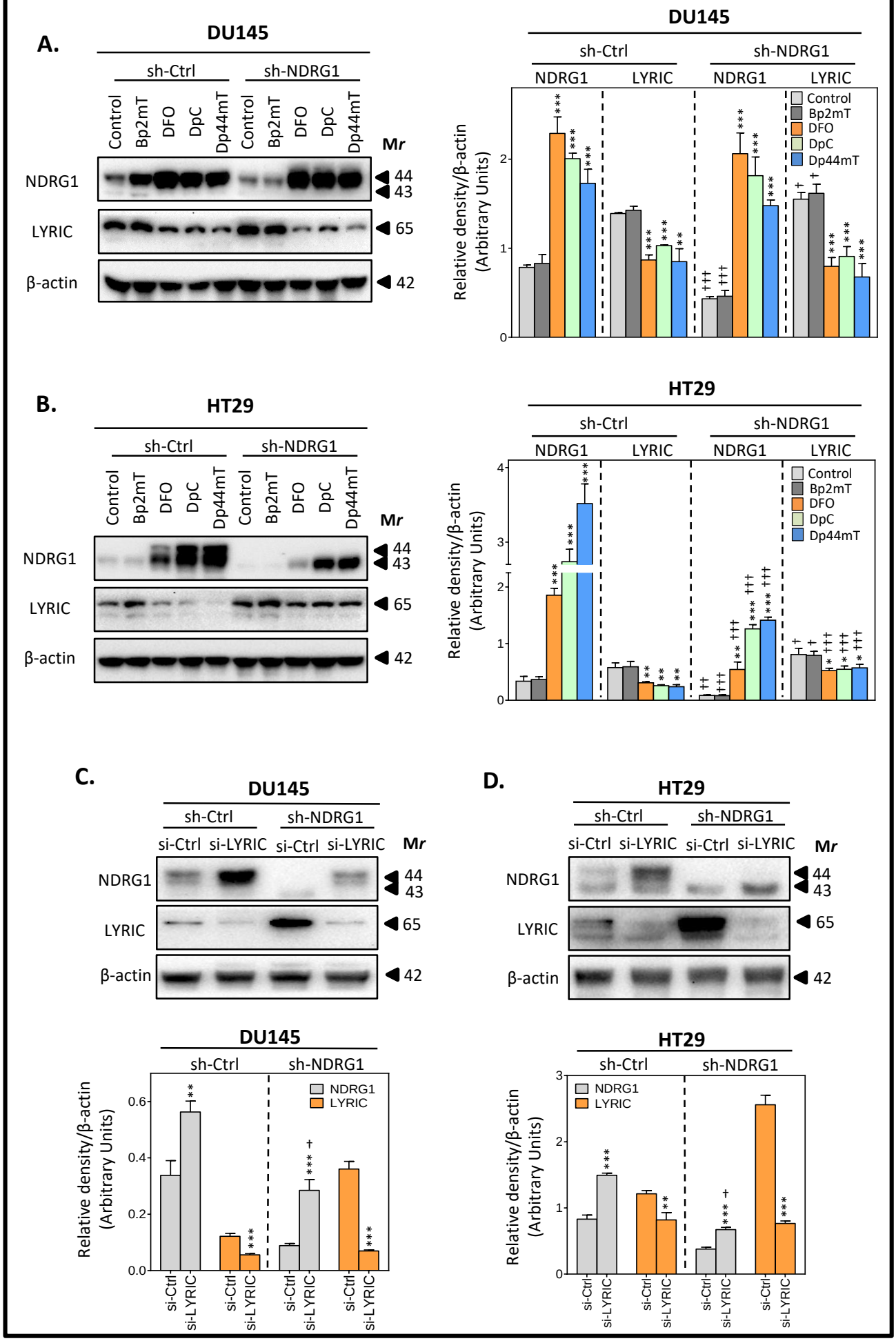
A.
DU145
sh-Ctrl
sh-NDRG1
Control
Bp2mT
DFO
DpC
Dp44mT
Mr
NDRG1
LYRIC
β-actin
44
43
65
42
Relative density/β-actin (Arbitrary Units)
B.
HT29
C.
si-Ctrl
si-LYRIC
D.

Figure 7

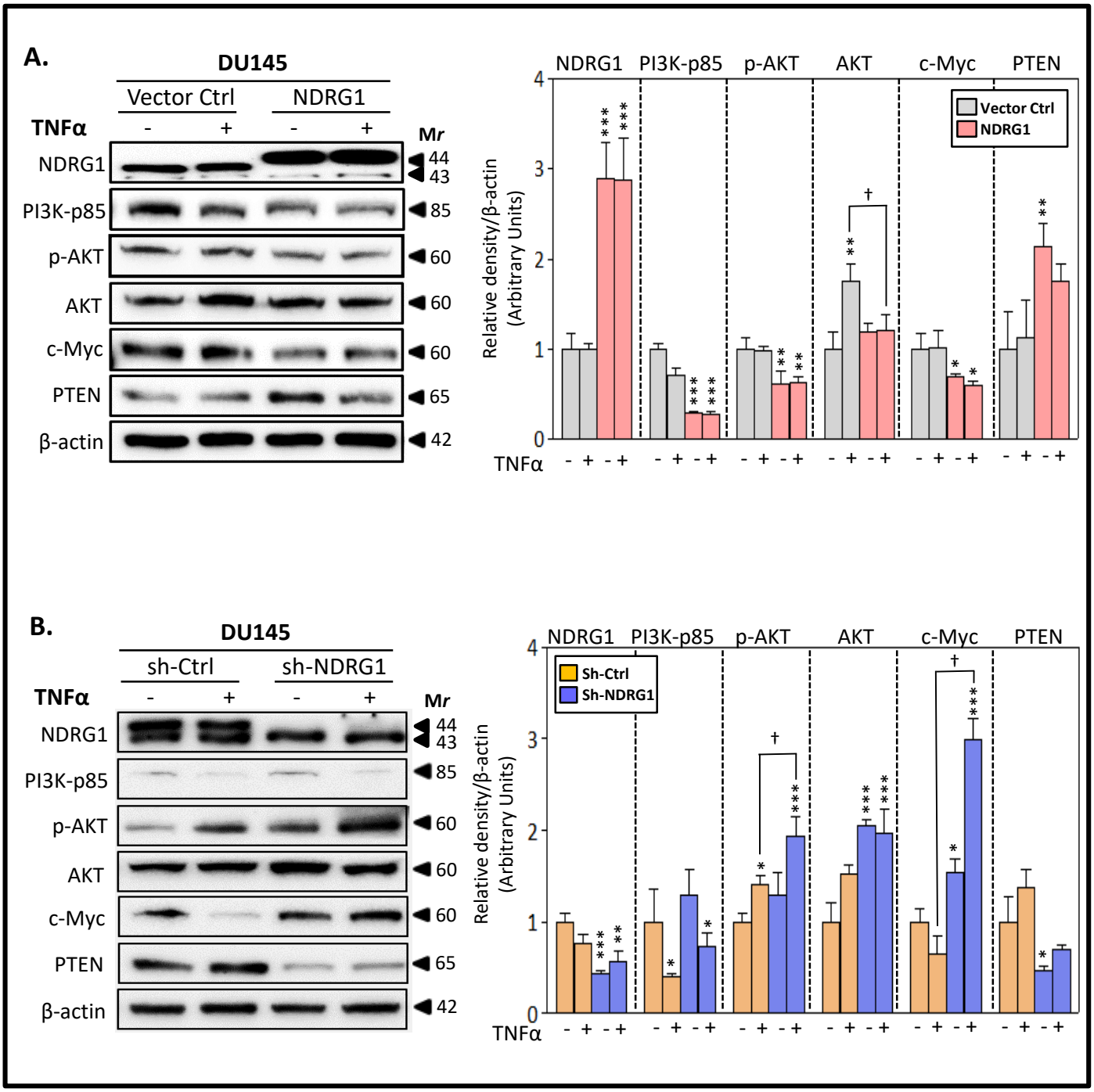
A.
DU145
Vector Ctrl
NDRG1
TNFα
- + - +
Mr
NDRG1
PI3K-p85
p-AKT
AKT
c-Myc
PTEN
β-actin
44
43
85
60
60
60
65
42
NDRG1 PI3K-p85 p-AKT AKT c-Myc PTEN
Vector Ctrl
NDRG1
Relative density/β-actin (Arbitrary Units)
TNFα
B.
DU145
sh-Ctrl
sh-NDRG1
Sh-Ctrl
Sh-NDRG1

Figure 8

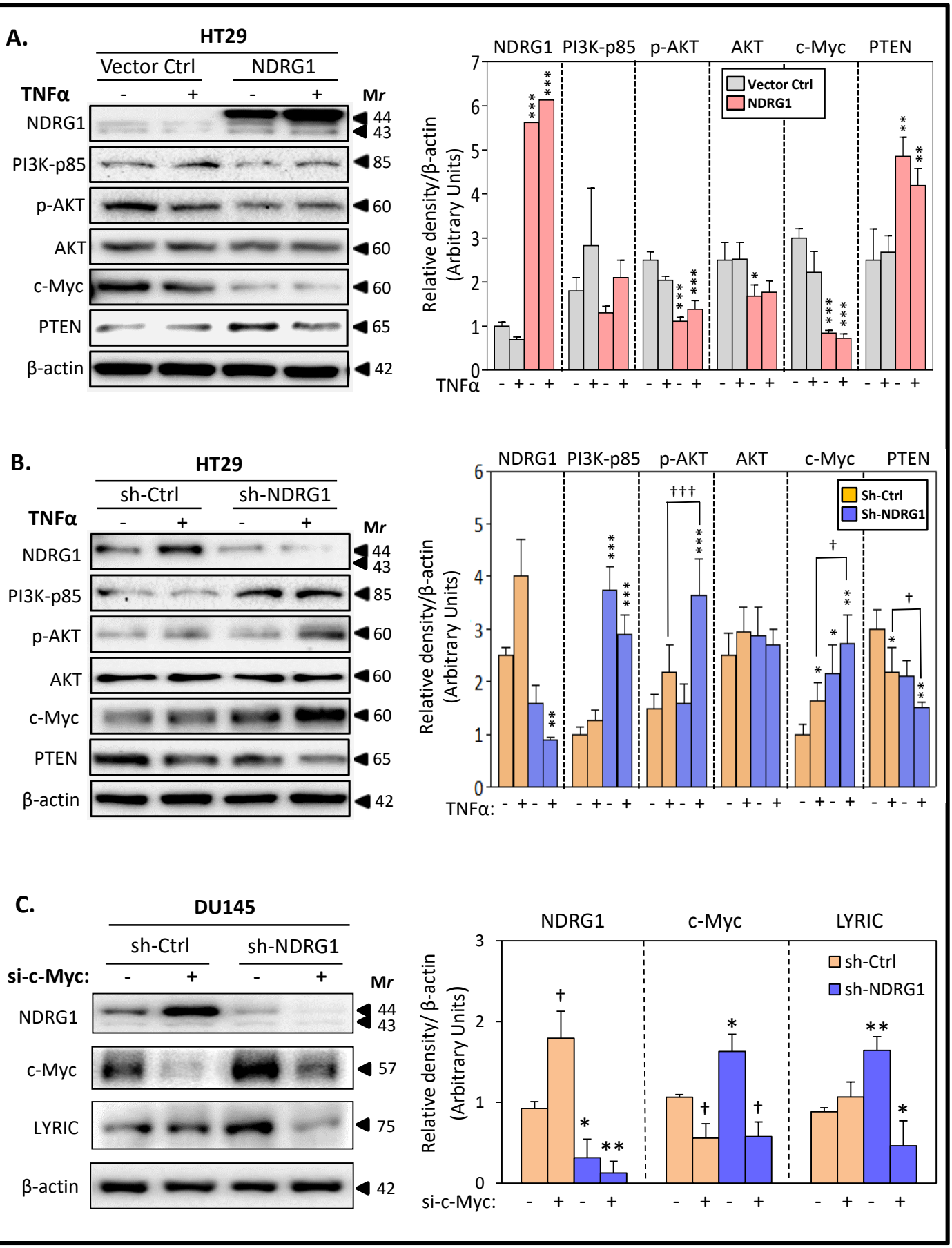
A.
HT29
Vector Ctrl
NDRG1
TNFα
- + - +
Mr
NDRG1
PI3K-p85
p-AKT
AKT
c-Myc
PTEN
β-actin
44
43
85
60
60
60
65
42
NDRG1 PI3K-p85 p-AKT AKT c-Myc PTEN
Vector Ctrl
NDRG1
Relative density/β-actin (Arbitrary Units)
TNFα
B.
HT29
sh-Ctrl
sh-NDRG1
TNFα
- + - +
Mr
NDRG1
PI3K-p85
p-AKT
AKT
c-Myc
PTEN
β-actin
44
43
85
60
60
60
65
42
NDRG1 PI3K-p85 p-AKT AKT c-Myc PTEN
Sh-Ctrl
Sh-NDRG1
Relative density/β-actin (Arbitrary Units)
TNFα:
C.
DU145
sh-Ctrl
sh-NDRG1
si-c-Myc:
- + - +
Mr
NDRG1
c-Myc
LYRIC
β-actin
44
43
57
75
42
NDRG1 c-Myc LYRIC
sh-Ctrl
sh-NDRG1
Relative density/ β-actin (Arbitrary Units)
si-c-Myc:

Figure 9

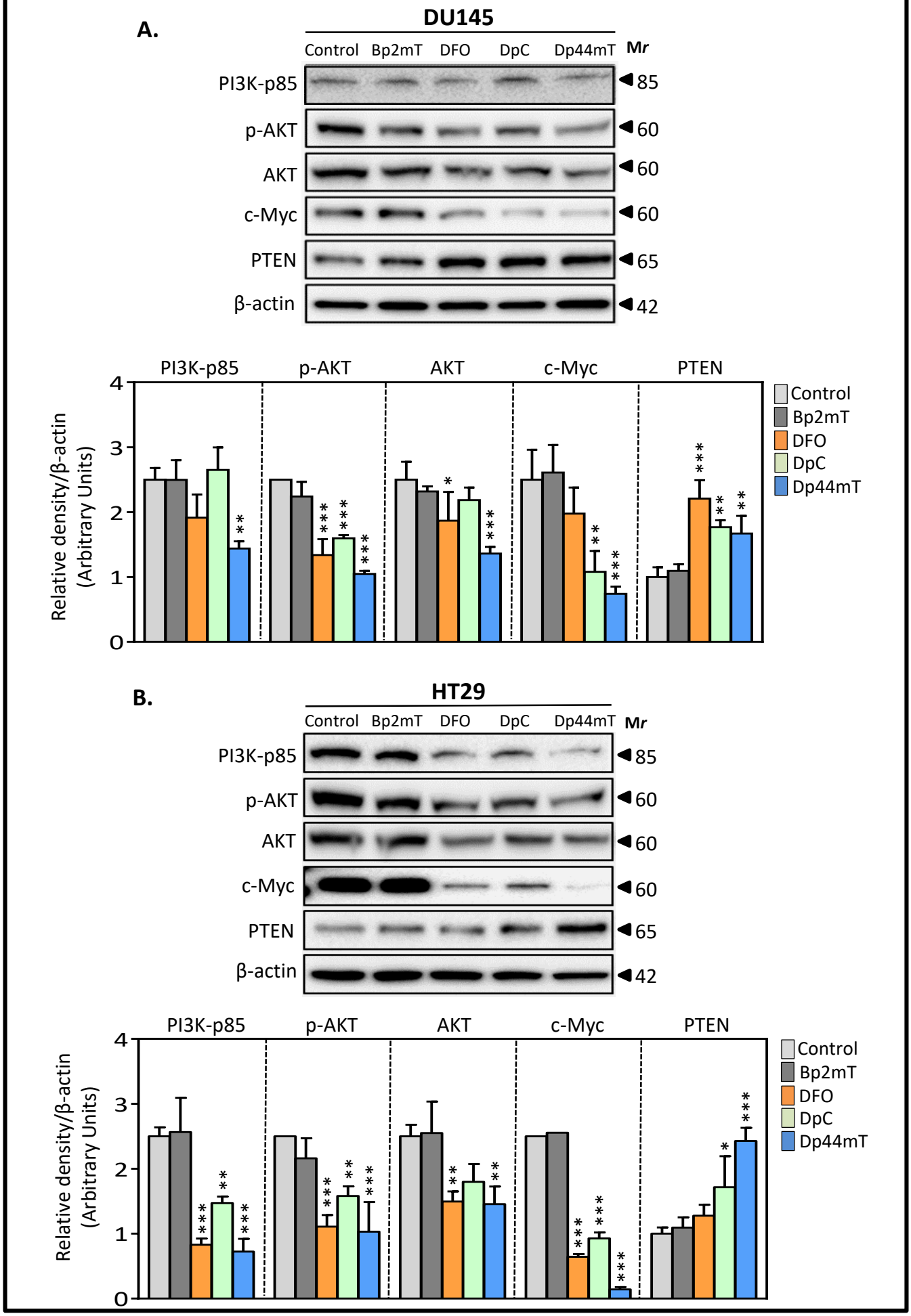
A.
DU145
Control
Bp2mT
DFO
DpC
Dp44mT
Mr
PI3K-p85
p-AKT
AKT
c-Myc
PTEN
β-actin
85
60
60
60
65
42
PI3K-p85
p-AKT
AKT
c-Myc
PTEN
Relative density/β-actin (Arbitrary Units)
Control
Bp2mT
DFO
DpC
Dp44mT
B.
HT29
Control
Bp2mT
DFO
DpC
Dp44mT
Mr
PI3K-p85
p-AKT
AKT
c-Myc
PTEN
β-actin
85
60
60
60
65
42
PI3K-p85
p-AKT
AKT
c-Myc
PTEN
Relative density/β-actin (Arbitrary Units)
Control
Bp2mT
DFO
DpC
Dp44mT

Figure 10

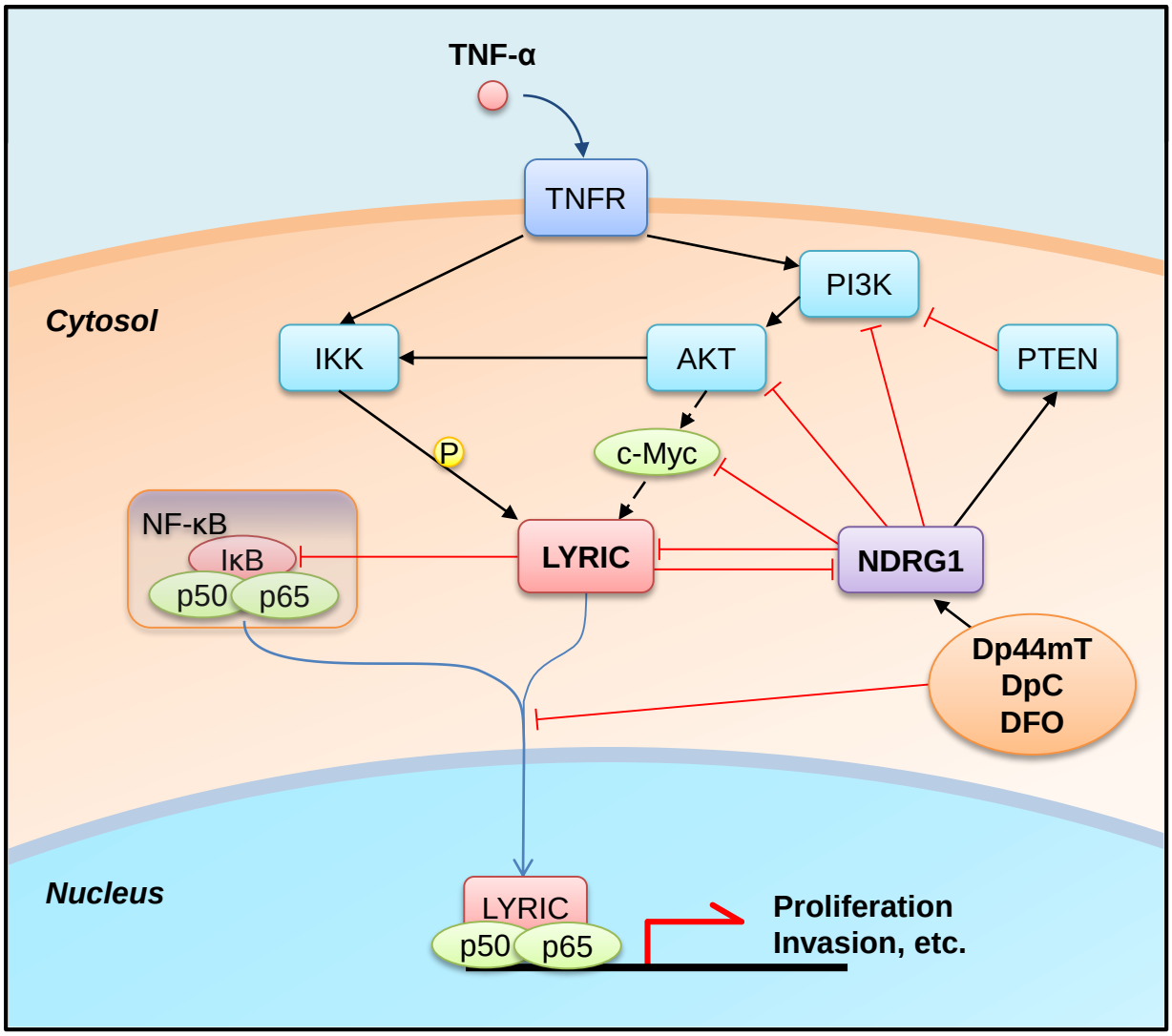
TNF-α
TNFR
PI3K
Cytosol
IKK
AKT
PTEN
P
c-Myc
NF-κB
IκB
p50
p65
LYRIC
NDRG1
Dp44mT
DpC
DFO
Nucleus
LYRIC
p50
p65
Proliferation
Invasion, etc.

Figure 11